



Contents lists available at ScienceDirect

## Spectrochimica Acta Part A: Molecular and Biomolecular Spectroscopy

journal homepage: [www.elsevier.com/locate/saa](http://www.elsevier.com/locate/saa)

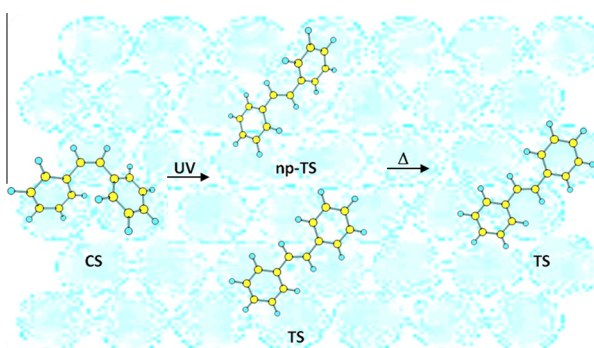
## Trans- and cis-stilbene isolated in cryogenic argon and xenon matrices

Ozan Ünsalan<sup>a,b</sup>, Nihal Kuş<sup>a,c</sup>, Susana Jarmelo<sup>a</sup>, Rui Fausto<sup>a,\*</sup><sup>a</sup> Department of Chemistry, University of Coimbra, P-3004-535 Coimbra, Portugal<sup>b</sup> Department of Physics, Faculty of Sciences, University of Istanbul, Turkey<sup>c</sup> Department of Physics, Anadolu University, Eskişehir, Turkey

## HIGHLIGHTS

- Monomers of *trans*- (TS) and *cis*-stilbene (CS) were isolated in cryogenic argon and xenon matrices.
- TS and CS infrared spectra were fully assigned and interpreted.
- *In situ* broadband UV irradiation of the matrix-isolated CS led to its isomerization to TS.
- TS appears in the photolysed matrices in both non-planar and planar configurations.
- Chemometrics was used to assign the structure of the non-planar TS form.

## GRAPHICAL ABSTRACT



## ARTICLE INFO

Article history:  
Available online xxxxx

Keywords:  
*Trans*- and *cis*-stilbene  
Matrix isolation IR spectroscopy  
DFT(B3LYP)/6-311++G(d,p) calculations  
*Cis* → *trans* photoisomerization

## ABSTRACT

Monomers of *trans*- (TS) and *cis*-stilbene (CS) were isolated in cryogenic argon and xenon matrices, and their infrared (IR) spectra were fully assigned and interpreted. The interpretation of the vibrational spectra received support from theoretical calculations undertaken at the DFT(B3LYP)/6-311++G(d,p) level of theory. *In situ* broadband UV irradiation of the matrix-isolated CS led to its isomerization to TS, which appeared in the photolysed matrices in both non-planar and planar configurations. The non-planar species was found to convert into the more stable planar form upon subsequent annealing of the matrices at higher temperature. TS was found to be photostable under the used experimental conditions. The structure of the non-planar TS form was assigned based on the comparison of its observed IR spectrum with those theoretically predicted for different conformations of TS. Chemometrics was used to make this assignment. Additional reasoning on the structure of the studied stilbenes is presented taking as basis results of the Natural Bond Orbital analysis.

© 2013 Elsevier B.V. All rights reserved.

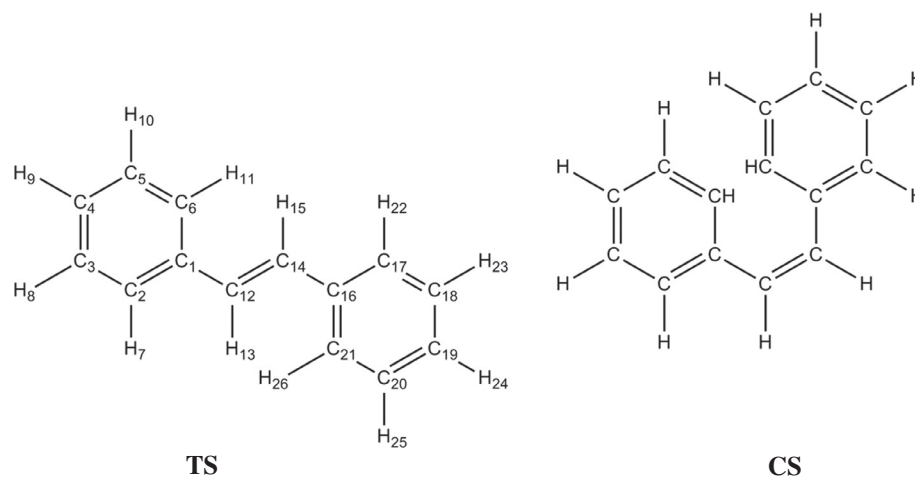
## Introduction

Stilbene exists as two possible stereoisomers about the double bond, *trans* (TS) and *cis* (CS) (Scheme 1). Being the simplest 1,2-diarylethylene, stilbene has been extensively used as a model system for investigation of the photochemical dynamics concerning the *cis* → *trans* isomerization about a C=C bond. This type of photoisomerization is of fundamental importance in many areas of chemistry, physics, biochemistry and materials science, and

along the years there has been a continuing interest in this topic [1–28].

CS is well-known to present a non-planar structure [29–32], due to the stress imposed by the presence of the two large phenyl substituents in the same side of the double bond. On the other hand, the structure of TS has been a source of controversy, because the two phenyl groups can rotate with a very low energy cost [33–44]. Electron diffraction and photoelectron spectroscopy studies on gaseous TS [33,34] suggested the molecule to be non-planar with phenyl groups rotated by ~30° around the C–phenyl bonds, in line with some theoretical results [43,44]. However, the most recent theoretical data favor the idea that TS has, as its minimum

\* Corresponding author. Tel.: +351 239 854483; fax: +351 239 827703.  
E-mail address: [rfausto@ci.uc.pt](mailto:rfausto@ci.uc.pt) (R. Fausto).



**Scheme 1.** *Trans*- (TS) and *cis*-stilbene (CS). Atom numbering adopted in this study.

energy structure, a strictly planar form [40,41]. This is in agreement with experimental results for the compound in molecular beams [45] (in solid state TS molecules were also found to exhibit a planar configuration [36,46–49], while in solution and liquid phase appear to be non-planar [50–52]). The better available estimations of the relative energies of the planar and  $\sim 30^\circ$  distorted geometries of TS, undertaken at CCSD/cc-pVDZ and Møller–Plesset levels of theory in conjunction with Dunning’s correlation consistent polarized valence basis sets [40,41], yielded values from 2 to  $\sim 0.4$  kJ mol $^{-1}$ , favoring the planar form. Moreover, it was also recently shown that zero-point-vibrational corrections are comparable to the energy increase between the planar and non-planar forms, so that this effect (“vibrational quasi-planarity” [40]) can be used to explain the controversy on the planar/non-planar conformational preferences of TS. A general consensus exists regarding the low energy – large amplitude nature of the C–phenyl torsional vibrations in TS [33–49].

As mentioned above, the *cis*  $\rightarrow$  *trans* photoisomerism in stilbene has been an area of intense study [1–28]. The photoisomerization has been explained as proceeding with the intermediacy of a non-planar excited state minimum and relaxation to the ground state through a conical intersection. A recent matrix isolation (argon, krypton and N $_2$  matrices) study of the *cis*  $\rightarrow$  *trans* photoisomerism in stilbene [53], successfully allowed observation of a non-planar form of the photoproducted TS.

In the present study, one intended to investigate in further detail the structure and vibrational spectra of matrix-isolated *trans*- and *cis*-stilbenes, and characterize better structurally and spectroscopically the non-planar TS form resulting from *cis*  $\rightarrow$  *trans* photoisomerization of stilbene in a cryogenic matrix. The studies were undertaken for the compounds isolated in argon matrices and, for the first time, also in xenon matrices.

## Experimental and computational methods

### Matrix isolation FTIR and photochemical experiments

*Trans*-stilbene (TS; *trans*-1,2-diphenylethylene) and *cis*-stilbene (CS; *cis*-1,2-diphenylethylene) were purchased from Sigma–Aldrich, purity  $\geq 96\%$ . To prepare the cryogenic matrices, the vapors of the studied compounds were deposited, together with a large excess of argon (N60) or xenon (N45) (both supplied by Air Liquide), onto a cryogenic CsI window, which was used as optical substrate. During deposition of the matrices, the temperature of the substrate was kept at 15 K. The temperature was directly

measured at the sample holder by a silicon diode sensor connected to a digital controller (Scientific Instruments, Model 9650-1), with an accuracy of 0.1 K. TS was sublimated ( $T \sim 50^\circ\text{C}$ ) from a miniature glass furnace placed in the vacuum chamber of the cryostat. CS was evaporated from a glass tube connected to the cryostat through a needle valve. Before cooling the cryostat, the glass tube was degassed to remove remaining air and volatile impurities. This allowed additional purification of the compound immediately before the experiment. The inert gases were used as supplied.

The matrices were irradiated for about 90 min through the outer KBr window ( $\lambda > 225$  nm) of the cryostat, with a HBO200 high-pressure mercury lamp. This lamp was fitted with a water filter to remove IR radiation. After irradiation, the matrices were annealed, with temperature steps of 3 K, up to 39 K (Ar), or steps of 5 K, until 80 K (Xe).

The low-temperature equipment was based on a closed-cycle helium refrigerator (APD Cryogenics) with a DE-202A expander. The IR spectra were recorded in the range 4000–400 cm $^{-1}$ , with a resolution of 0.5 cm $^{-1}$ , using a Thermo Nicolet 6700 Fourier-transform infrared (FTIR) spectrometer, equipped with a KBr beam splitter and a deuterated triglycine sulfate (DTGS) detector.

### Theoretical calculations

All theoretical calculations were performed using the Gaussian 03 program package [54] at the DFT(B3LYP) level of theory [55,56], with the 6-311++G(d,p) basis set [57]. Natural bond orbital (NBO) analysis was performed according to Weinhold and co-workers [58,59] using NBO 3 as implemented in Gaussian 03. Calculated harmonic vibrational wavenumbers were scaled down by a single factor of 0.978, to correct them for the systematic shortcomings of the applied methodology (mainly for anharmonicity). The theoretical normal modes were analyzed by carrying out the potential energy distribution (PED) calculations, as described by Schachtschneider and Mortimer [60]. Chemometrics analyses were undertaken using R package “stats” (version 2.15.3) [61].

## Results and discussion

### IR spectra of TS and CS monomers isolated in argon and xenon matrices

Infrared spectra of matrix-isolated TS and CS are shown in Figs. 1 and 2, where they are compared with the corresponding DFT(B3LYP)/6-311++G(d,p) calculated spectra. The detailed

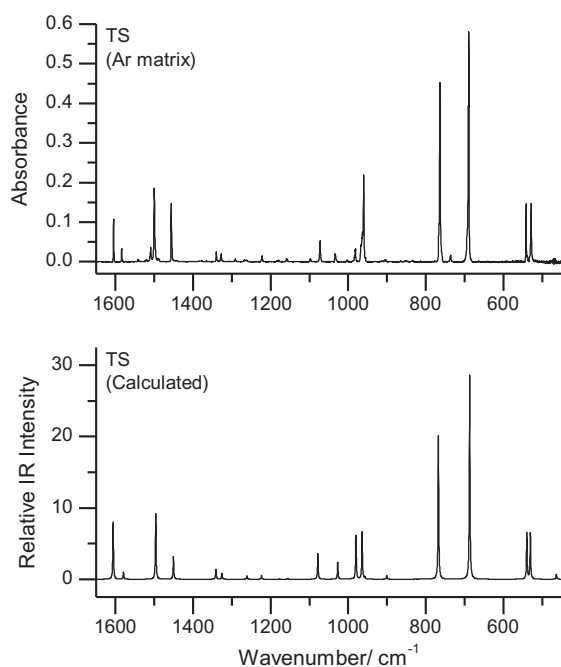


**Fig. 1.** Top: Infrared spectrum of *trans*-stilbene isolated in argon matrix ( $T = 15$  K;  $1650\text{--}450\text{ cm}^{-1}$  range); Bottom: B3LYP/6-311++G(d,p) calculated infrared spectrum of *trans*-stilbene (wavenumbers scaled by 0.978; the bands were simulated using Lorentzian functions with full widths at half-maximum-height (fwhm) of  $2\text{ cm}^{-1}$  centered at the scaled wavenumbers; the calculated intensities correspond to the area below the peaks).

assignment of these spectra and the results of the normal mode analyses are given in Tables 1 and 2. The definitions of the symmetry coordinates used in the normal coordinate analyses are provided in Table S1 (Supporting Information).

As it can be noticed in Figs. 1 and 2, the theoretical calculations reproduce very well the experimental data. This allows a reliable assignment of the experimental IR bands. The sets of bands observed in the  $3130\text{--}3000\text{ cm}^{-1}$  and  $2000\text{--}1650\text{ cm}^{-1}$  wavenumber ranges originate in C–H stretching vibrations of both phenyl rings and ethylenic group and overtones/combination modes, respectively. As usually observed for matrix-isolation IR spectra, intensities of the C–H stretching bands are generally smaller than predicted by the calculations, making difficult a detailed assignment of the bands in the  $3130\text{--}3000\text{ cm}^{-1}$  range. Because of that, these bands were not used either in the scaling of the calculated intensities shown in Tables 1 and 2 or in the chemometrics studies, described in the next section, which were performed to establish similarities between the observed spectra of the photoproducts of CS and the calculated spectra for different non-planar TS configurations. Below, we will center our discussion on the most prominent observed fundamental bands appearing below  $1650\text{ cm}^{-1}$ .

#### IR spectrum of matrix-isolated *trans*-stilbene ( $C_{2h}$ )

Planar *trans*-stilbene belongs to the  $C_{2h}$  point group, so that only  $A_u$  and  $B_u$  symmetry type vibrations are infrared active.

The three most intense bands observed in the  $1650\text{--}1400\text{ cm}^{-1}$  wavenumber range, whose maxima are located at  $1605$ ,  $1500$  and  $1456\text{ cm}^{-1}$  (in argon matrix;  $1602$ ,  $1498$  and  $1454\text{ cm}^{-1}$  in xenon) are due to vibrations of the phenyl rings, the first being a CC ring stretching mode [ $\nu(\text{CC})_{3b}$ ; see Table 1] and the two last corresponding mostly to in-plane CH ring deformations [ $\delta(\text{CH})_{4b}$ ;  $\delta(\text{CH})_{5b}$ ] and exhibiting multiplet structure due to matrix-site splitting. The ethylenic C=C stretching belongs to the  $A_g$  symmetry species and is IR inactive.

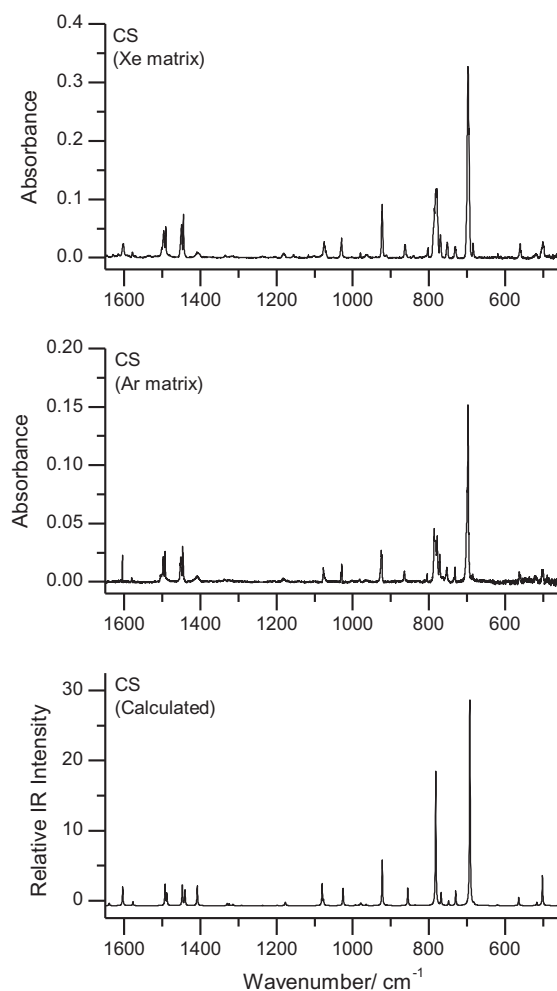


**Fig. 2.** Top and middle: Infrared spectra of *cis*-stilbene isolated in xenon and argon matrices ( $T = 15$  K;  $1650\text{--}450\text{ cm}^{-1}$  range); Bottom: B3LYP/6-311++G(d,p) calculated infrared spectrum of *cis*-stilbene (wavenumbers scaled by 0.978; the bands were simulated using Lorentzian functions with full widths at half-maximum-height (fwhm) of  $2\text{ cm}^{-1}$  centered at the scaled wavenumbers; the calculated intensities correspond to the area below the peaks).

In the  $1400\text{--}800\text{ cm}^{-1}$  wavenumber range several low intensity bands appear. The most intense band in this spectral region is predicted by the calculations at  $964\text{ cm}^{-1}$  and was observed as a site-split multiplet with main components at  $\sim 960\text{ cm}^{-1}$  in argon matrix, and as a doublet of bands at  $960/958\text{ cm}^{-1}$  in xenon. These features are assigned to the out of plane symmetric mode of the ethylenic moiety [ $\gamma_s(\text{=CH})$ ]. Two additional bands with medium intensity were predicted to occur in this spectral region at  $1078\text{ cm}^{-1}$  [ring stretching  $\nu(\text{CC})_{5b}$ ] and  $980\text{ cm}^{-1}$  [ring out of plane  $\gamma(\text{CH})_{5a}$ ]. The corresponding observed features are observed at  $1073$  and around  $980\text{ cm}^{-1}$  (the last as a triplet) in argon matrix, and at  $1075/1070$  and  $979\text{ cm}^{-1}$  in xenon.

The two strong calculated bands at  $768$  and  $687\text{ cm}^{-1}$  are associated with the all-in-phase symmetric out of plane  $\gamma(\text{CH})_{1a}$  phenyl bending mode and the  $\tau(\text{Ph})_{1a}$  torsional mode that distorts the phenyl rings towards cyclohexane chair-type conformations, respectively. Experimentally, these vibrations were found to give rise to the two most intense observed IR bands of TS, the first one as a triplet of bands (argon:  $766/764/763\text{ cm}^{-1}$ ; xenon:  $771/765/761\text{ cm}^{-1}$ ), and the second as a doublet (argon:  $690/689\text{ cm}^{-1}$ ; xenon:  $695/687\text{ cm}^{-1}$ ). For frequencies below that of the  $\tau(\text{Ph})_{1a}$  torsional mode only two bands were observed, corresponding to a deformational

**Table 1**  
Observed (argon matrix; 15 K; xenon matrix; 15 K) and calculated (B3LYP/6-311++G(d,p)) IR spectra and potential energy distribution of the normal modes (PED,%) for *trans*-stilbene (C<sub>2h</sub>).<sup>a</sup>

Approximate description	PED	Symmetry	Calculated		Observed (Ar) <sup>b</sup>				Observed (Xe) <sup>b</sup>				
			$\nu$	$I$	$\nu$	$I$	$\nu^{bc}$	$I^{bc}$	$\nu$	$I$	$\nu^{bc}$	$I^{bc}$	
$\nu(\text{CH})_{1a}$	S <sub>2</sub> [86]	A <sub>g</sub>	3121.0	0.0									
$\nu(\text{CH})_{1b}$	S <sub>38</sub> [86]	B <sub>u</sub>	3120.8	37.4	3112.9	1.0	3109.0	2.0	3102.9	3.2	3102.9	3.2	
					3105.0	1.0							
$\nu(\text{CH})_{3b}$	S <sub>40</sub> [74]	B <sub>u</sub>	3113.4	52.8	3094.0	2.1	3089.5	7.7	3078.5	7.5	3078.5	7.5	
					3090.8	2.9							
					3084.6	2.7							
$\nu(\text{CH})_{3a}$	S <sub>4</sub> [74]	A <sub>g</sub>	3113.2	0.0									
$\nu(\text{CH})_{5a}$	S <sub>6</sub> [67] + S <sub>3</sub> [23]	A <sub>g</sub>	3104.4	0.0									
$\nu(\text{CH})_{5b}$	S <sub>42</sub> [67] + S <sub>39</sub> [23]	B <sub>u</sub>	3104.1	23.4	3069.5	3.4	3069.5	3.4	3054.7	5.0	3054.7	5.0	
$\nu(\text{CH})_{2b}$	S <sub>39</sub> [50] + S <sub>40</sub> [20] + S <sub>42</sub> [14] + S <sub>41</sub> [10]	B <sub>u</sub>	3094.6	0.3					n.obs.				
$\nu(\text{CH})_{2a}$	S <sub>3</sub> [53] + S <sub>4</sub> [24] + S <sub>6</sub> [14]	A <sub>g</sub>	3094.2	0.0									
$\nu(\text{CH})_{4a}$	S <sub>5</sub> [81]	B <sub>u</sub>	3087.7	22.8	3037.7	6.4	3037.7	6.4	3024.1	2.3	3024.1	2.3	
$\nu(\text{CH})_{4b}$	S <sub>41</sub> [78] + S <sub>39</sub> [13]	A <sub>g</sub>	3087.6	0.0									
$\nu_{as}(=\text{CH})$	S <sub>43</sub> [91]	B <sub>u</sub>	3075.8	23.1					3014.9	3.8	3014.9	3.8	
$\nu_s(=\text{CH})$	S <sub>7</sub> [94]	A <sub>g</sub>	3067.2	0.0									
$\nu(\text{C}=\text{C})$	S <sub>1</sub> [55] + S <sub>24</sub> [22]	A <sub>g</sub>	1647.9	0.0									
$\nu(\text{CC})_{3b}$	S <sub>46</sub> [66] + S <sub>53</sub> [21]	B <sub>u</sub>	1606.1	25.4	1605.0	9.8	1605.0	9.8	1602.0	11.2	1602.0	11.2	
$\nu(\text{CC})_{3a}$	S <sub>10</sub> [63] + S <sub>17</sub> [21]	A <sub>g</sub>	1597.3	0.0									
$\nu(\text{CC})_{4b}$	S <sub>47</sub> [66] + S <sub>52</sub> [17]	B <sub>u</sub>	1579.5	3.0	1584.3	2.9	1584.3	2.9	1581.2	8.1	1581.2	8.1	
$\nu(\text{CC})_{4a}$	S <sub>11</sub> [63] + S <sub>16</sub> [19]	A <sub>g</sub>	1574.1	0.0									
$\delta(\text{CH})_{4b}$	S <sub>54</sub> [59] + S <sub>49</sub> [32]	B <sub>u</sub>	1496.4	29.0	1509.5	3.2	1501.9	20.0	1505.5	0.6	1498.1	8.1	
					1500.4	16.8			1497.5	7.5			
$\delta(\text{CH})_{4a}$	S <sub>18</sub> [63] + S <sub>13</sub> [32]	A <sub>g</sub>	1488.2	0.0									
$\delta(\text{CH})_{5b}$	S <sub>48</sub> [26] + S <sub>55</sub> [23] + S <sub>52</sub> [15] + S <sub>51</sub> [13]	B <sub>u</sub>	1450.7	10.1	1456.3	13.3	1455.6	18.0	1453.6	30.3	1451.8	36.8	
					1454.6	4.0			1451.5	1.4			
					1449.7	0.4			1445.7	1.8			
					1442.6	0.3			1438.8	3.3			
$\delta(\text{CH})_{5a}$	S <sub>19</sub> [26] + S <sub>12</sub> [20] + S <sub>15</sub> [17] + S <sub>9</sub> [13] + S <sub>16</sub> [11]	A <sub>g</sub>	1442.6	0.0									
$\delta(\text{CH})_{1b}$	S <sub>51</sub> [45] + S <sub>60</sub> [35]	B <sub>u</sub>	1341.1	4.5	1340.5	2.2	1340.5	2.2	1338.6	3.9	1338.6	3.9	
$\delta(\text{CH})_{1a}$	S <sub>15</sub> [58] + S <sub>24</sub> [19]	A <sub>g</sub>	1334.9	0.0									
$\nu(\text{CC})_{2b}$	S <sub>45</sub> [60] + S <sub>51</sub> [32] + S <sub>55</sub> [12]	B <sub>u</sub>	1325.4	2.6	1327.5	1.7	1327.5	1.7	1326.3	5.4	1326.3	5.4	
$\delta_s(=\text{CH})$	S <sub>24</sub> [42] + S <sub>9</sub> [28] + S <sub>15</sub> [14] + S <sub>1</sub> [14]	A <sub>g</sub>	1320.0	0.0									
$\nu(\text{CC})_{2a}$	S <sub>9</sub> [41] + S <sub>11</sub> [19] + S <sub>25</sub> [10]	A <sub>g</sub>	1299.8	0.0									
$\nu_{as}(\text{C}-\text{C})$	S <sub>50</sub> [34] + S <sub>48</sub> [12] + S <sub>45</sub> [10]	B <sub>u</sub>	1261.4	1.5	1267.3	0.5	1265.1	0.9	1265.8	1.8	1265.8	1.8	
					1262.3	0.4							
$\delta_{as}(=\text{CH})$	S <sub>60</sub> [35] + S <sub>50</sub> [14] + S <sub>45</sub> [10]	B <sub>u</sub>	1223.6	1.8	1224.5	0.4	1222.7	1.7	1223.9	1.9	1223.9	1.9	
					1222.2	1.3							
$\nu_s(\text{C}-\text{C})$	S <sub>14</sub> [23] + S <sub>17</sub> [13] + S <sub>8</sub> [11] + S <sub>21</sub> [10]	A <sub>g</sub>	1184.7	0.0									
$\delta(\text{CH})_{3a}$	S <sub>17</sub> [62] + S <sub>10</sub> [16]	A <sub>g</sub>	1179.6	0.0									
$\delta(\text{CH})_{3b}$	S <sub>53</sub> [73] + S <sub>66</sub> [21]	B <sub>u</sub>	1178.0	0.2	1183.5	0.3	1181.2	0.6	1178.4	1.3	1178.4	1.3	
					1179.5	0.3							
$\delta(\text{CH})_{2a}$	S <sub>16</sub> [42] + S <sub>19</sub> [38] + S <sub>9</sub> [12]	A <sub>g</sub>	1156.5	0.0									
$\delta(\text{CH})_{2b}$	S <sub>52</sub> [40] + S <sub>55</sub> [40] + S <sub>45</sub> [12]	B <sub>u</sub>	1156.1	0.4	1159.1	0.7	1158.5	1.3	1155.4	1.4	1155.4	1.4	
					1157.7	0.6							
$\nu(\text{CC})_{5a}$	S <sub>12</sub> [48] + S <sub>19</sub> [22] + S <sub>16</sub> [17]	A <sub>g</sub>	1081.1	0.0									
$\nu(\text{CC})_{5b}$	S <sub>48</sub> [56] + S <sub>55</sub> [21] + S <sub>52</sub> [17]	B <sub>u</sub>	1078.3	11.4	1072.6	4.7	1072.6	4.7	1075.0	2.8	1071.0	11.2	
									1069.7	8.4			
$\nu(\text{CC})_{6b}$	S <sub>49</sub> [52] + S <sub>54</sub> [23] + S <sub>44</sub> [20]	B <sub>u</sub>	1027.0	7.6	1034.2	1.8	1034.2	1.8	1031.5	4.6	1031.5	4.6	
$\nu(\text{CC})_{6a}$	S <sub>13</sub> [48] + S <sub>8</sub> [23] + S <sub>18</sub> [21]	A <sub>g</sub>	1025.3	0.0									
$\delta(\text{Ph})_{1b}$	S <sub>57</sub> [67] + S <sub>44</sub> [32]	B <sub>u</sub>	991.7	0.2	988.4	0.2	988.4	0.2	n.obs.				
$\delta(\text{Ph})_{1a}$	S <sub>21</sub> [61] + S <sub>8</sub> [37]	A <sub>g</sub>	990.9	0.0									
$\gamma(\text{CH})_{5a}$	S <sub>30</sub> [65] + S <sub>32</sub> [49]	A <sub>u</sub>	980.1	19.4	982.0	2.7	981.3	6.3	978.8	13.9	978.8	13.9	
					981.1	2.9							
					979.6	0.7							
$\gamma(\text{CH})_{5b}$	S <sub>66</sub> [100]	B <sub>g</sub>	972.6	0.0									
$\gamma_s(=\text{CH})$	S <sub>32</sub> [52] + S <sub>30</sub> [49] + S <sub>27</sub> [10]	A <sub>u</sub>	964.3	20.8	966.3	4.0	961.5	61.7	960.3	6.5	958.0	43.7	
					964.4	5.5			957.6	37.2			
					963.6	6.8							
					961.4	9.0							
					960.4	16.5							
					959.9	19.7							
$\gamma(\text{CH})_{4a}$	S <sub>29</sub> [100]	A <sub>u</sub>	957.3	0.8	n.obs.				n.obs.				
$\gamma(\text{CH})_{4b}$	S <sub>65</sub> [100]	B <sub>g</sub>	956.7	0.0									
$\gamma(\text{CH})_{2b}$	S <sub>63</sub> [56] + S <sub>68</sub> [26] + S <sub>67</sub> [14]	B <sub>g</sub>	910.3	0.0									
$\gamma(\text{CH})_{2a}$	S <sub>27</sub> [86]	A <sub>u</sub>	900.7	1.7	904.6	0.5	904.6	0.5	906.1	0.9	906.1	0.9	
$\nu(\text{CC})_{1a}$	S <sub>25</sub> [30] + S <sub>8</sub> [20] + S <sub>14</sub> [13] + S <sub>21</sub> [11]	A <sub>g</sub>	861.7	0.0									
$\gamma_{as}(=\text{CH})$	S <sub>68</sub> [45] + S <sub>63</sub> [39] + S <sub>64</sub> [12]	B <sub>g</sub>	860.6	0.0									
$\gamma(\text{CH})_{3a}$	S <sub>28</sub> [99]	A <sub>u</sub>	827.1	0.2	833.5	0.2	833.5	0.2	821.7	0.5	821.7	0.5	
$\gamma(\text{CH})_{3b}$	S <sub>64</sub> [83]	B <sub>g</sub>	825.9	0.0									
$\nu(\text{CC})_{1b}$	S <sub>44</sub> [31] + S <sub>50</sub> [27] + S <sub>57</sub> [16] + S <sub>58</sub> [11] + S <sub>49</sub> [10]	B <sub>u</sub>	814.7	0.1	812.9	0.1	812.9	0.1	808.6	1.9	808.6	1.9	
$\gamma(\text{CH})_{1a}$	S <sub>26</sub> [37] + S <sub>34</sub> [32] + S <sub>31</sub> [23] + S <sub>27</sub> [10]	A <sub>u</sub>	767.5	63.1	766.0	8.6	763.7	86.3	771.0	6.5	762.6	75.3	

(continued on next page)

					763.7	40.7			764.6	9.3		
					763.1	37.0			761.4	59.5		
$\gamma(\text{CH})_{1b}$	$S_{62}[60] + S_{69}[22]$	$B_g$	733.4	0.0								
$\tau(\text{Ph})_{1a}$	$S_{34}[62] + S_{26}[48]$	$A_u$	686.9	90.2	690.1	35.3	689.5	87.6	694.7	1.9	687.4	64.2
					689.1	52.3			687.2	62.3		
$\tau(\text{Ph})_{1b}$	$S_{69}[88] + S_{62}[27]$	$B_g$	684.0	0.0								
$\delta(\text{Ph})_{2a}$	$S_{22}[63] + S_{25}[21]$	$A_g$	640.6	0.0								
$\delta(\text{Ph})_{3b}$	$S_{59}[85]$	$B_u$	622.1	0.02	n.obs.				n.obs.			
$\delta(\text{Ph})_{3a}$	$S_{23}[86]$	$A_g$	618.6	0.0								
$\delta(\text{Ph})_{2b}$	$S_{58}[78]$	$B_u$	539.5	20.3	541.4	13.3	541.4	13.3	540.5	13.9	540.5	13.9
$\gamma_s(\text{Ph}-\text{C})$	$S_{31}[33] + S_{34}[23] + S_{36}[19] + S_{33}[16]$	$A_u$	530.4	20.4	528.3	13.3	528.3	13.3	526.4	23.2	526.4	23.2
$\tau(\text{Ph})_{3b}$	$S_{71}[42] + S_{67}[38] + S_{70}[12]$	$B_g$	465.6	0.0								
$w_{as}(\text{Ph}-\text{C})$	$S_{56}[57] + S_{61}[24] + S_{48}[11]$	$B_u$	463.4	2.2	467.2	0.7	467.2	0.7	n.obs.			
$\tau(\text{Ph})_{2a}$	$S_{35}[78] + S_{36}[36]$	$A_u$	402.9	0.006								
$\tau(\text{Ph})_{2b}$	$S_{70}[85] + S_{71}[29]$	$B_g$	402.4	0.0								
$w_s(\text{Ph}-\text{C})$	$S_{20}[48] + S_{14}[13] + S_{22}[13]$	$A_g$	281.3	0.0								
$\tau(\text{Ph})_{3a}$	$S_{36}[50] + S_{33}[28] + S_{35}[25]$	$A_u$	279.3	0.02								
$\gamma_{as}(\text{Ph}-\text{C})$	$S_{67}[37] + S_{71}[30] + S_{70}[16]$	$B_g$	215.3	0.0								
$\delta_s(\text{C}=\text{C}=\text{C})$	$S_{20}[35] + S_{25}[28] + S_{14}[19]$	$A_g$	200.4	0.0								
$\delta_{as}(\text{C}=\text{C}=\text{C})$	$S_{61}[72] + S_{56}[26]$	$B_u$	78.8	0.2								
$\tau_{as}(\text{C}-\text{C})$	$S_{72}[82] + S_{71}[11]$	$B_g$	75.8	0.0								
$\tau(\text{C}=\text{C})$	$S_{33}[56] + S_{31}[34]$	$A_u$	58.1	0.5								
$\tau_s(\text{C}-\text{C})$	$S_{37}[96]$	$A_u$	16.0	0.001								

<sup>a</sup> See Table S1 (Supporting information) for definition of symmetry coordinates;  $\nu$ , stretching;  $\delta$ , in-plane bending;  $w$ , wagging;  $\gamma$ , out-of-plane bending;  $\tau$ , torsion;  $s$ , symmetric;  $as$ , asymmetric; Ph, phenyl; n.obs., not observed; calculated wavenumbers ( $\text{cm}^{-1}$ ) were scaled by 0.978; calculated infrared intensities in  $\text{km mol}^{-1}$ ; PED's smaller than 10% are not given.

<sup>b</sup> Observed absorbances were normalized so that the total infrared intensity of the experimental bands (excluding those of the CH stretching bands) equals the corresponding calculated intensity (for experimental CH stretchings intensities, the same normalizing factor obtained was applied); the gravity centre (gc) of a given band was calculated as the intensity averaged mean wavenumber for the band components ascribed to a given vibration.

phenyl ring mode [ $\delta(\text{Ph})_{2b}$ ] ( $\sim 540 \text{ cm}^{-1}$ ) and the butterfly-type vibration of the molecule [ $\gamma_s(\text{Ph}-\text{C})$ ] (ca.  $530 \text{ cm}^{-1}$ ).

#### IR spectrum of matrix-isolated *cis*-stilbene ( $C_2$ )

*Cis*-stilbene belongs to the  $C_2$  point group and all vibrations are IR active. However, in spite of the different symmetries of TS and CS (and considerably larger number of IR active bands in CS), the spectra of both isomers are very similar, since in CS most of the vibrations appear as closely located pairs (with a  $B$  and an  $A$  symmetry type component resulting from symmetric and anti-symmetric combinations of similar vibrations of the two phenyl rings).

As for TS, the  $\nu(\text{CC})_{3b}$ ,  $\delta(\text{CH})_{4b}$  and  $\delta(\text{CH})_{5b}$  vibrations are predicted to give rise to relatively intense bands in the  $1650\text{--}1400 \text{ cm}^{-1}$  wavenumber range. The calculated frequencies for these modes are 1604, 1493 and  $1448 \text{ cm}^{-1}$ , which have experimental counterparts at 1605, 1498 (with 3 more weak components at slightly higher frequencies) and  $1454/1452 \text{ cm}^{-1}$  in argon, and at 1603, 1502/1496 and  $1450 \text{ cm}^{-1}$  in xenon, respectively. In this spectral range, CS also shows a relatively intense band due to the anti-symmetric in-plane CH ethylenic bending mode [ $\delta_{as}(\text{=CH})$ ], which is predicted to occur at  $1408 \text{ cm}^{-1}$  and was observed as a triplet of bands at 1411/1409/1406  $\text{cm}^{-1}$  in argon matrix and as a doublet at 1409/1406  $\text{cm}^{-1}$  in xenon.

In the  $1400\text{--}800 \text{ cm}^{-1}$  wavenumber range, the IR spectrum of CS is (like for TS) composed essentially by bands of very low intensity. In this range, only four bands have medium intensity. These bands are predicted by the calculations at 1080 [phenyl stretching  $\nu(\text{CC})_{5b}$ ], 1026 [phenyl stretching  $\nu(\text{CC})_{6b}$ ], 922 [phenyl out of plane  $\gamma(\text{CH})_{2b}$ ] and  $855 \text{ cm}^{-1}$  [phenyl stretching  $\nu(\text{CC})_{1b}$ ]. In argon matrix, they were observed at 1077/1075, 1029, triplet in the 925–923 range, and  $864 \text{ cm}^{-1}$ , while the corresponding bands in xenon appear at 1075/1073, 1029, triplet in the 924–916 range and  $862 \text{ cm}^{-1}$ . Contrarily to what happens for TS, the out of plane symmetric mode of the ethylenic moiety [ $\gamma_s(\text{=CH})$ ] is predicted by the calculations to have a low IR intensity ( $0.5 \text{ km mol}^{-1}$ ) and was not observed experimentally.

The most intense IR bands of CS are calculated to occur at 782 and  $692 \text{ cm}^{-1}$ . They correspond to the out of plane anti-symmetric mode of the ethylenic moiety [ $\gamma_{as}(\text{=CH})$ ] and to the all-in-phase anti-symmetric out of plane  $\gamma(\text{CH})_{1b}$  phenyl bending. The last

mode is also predicted to be almost coincident with the relatively intense band due to the  $\tau(\text{Ph})_{1a}$  torsional mode in CS. The theoretical predictions fit the experimental observations quite well. Accordingly, the  $\gamma_{as}(\text{=CH})$  mode was found to give rise to the intense multiplet-type band between 786 and  $778 \text{ cm}^{-1}$  (in argon matrix; between 788 and  $777 \text{ cm}^{-1}$  in xenon), and the  $\gamma(\text{CH})_{1b}$  vibration was found to be in the origin of the most intense experimental band, observed as an overlapped triplet feature at 702/699/697  $\text{cm}^{-1}$  and 698/697/695  $\text{cm}^{-1}$  in argon and xenon matrices, respectively. In turn,  $\tau(\text{Ph})_{1a}$  can be ascribed to the shoulders at 695 and  $693 \text{ cm}^{-1}$ , respectively in the argon and xenon matrix spectra. For frequencies below these last, only two mid intensity bands were expected at ca. 502 [ $\delta(\text{Ph})_{2b}$ ] and  $446 \text{ cm}^{-1}$  [ $\tau(\text{Ph})_{3b}$ ]. In argon matrix, these bands were observed at 503/500 and  $449 \text{ cm}^{-1}$ , while in xenon they correspond to site-splitting multiplet-type bands in the 505–498 and 447–442  $\text{cm}^{-1}$  ranges.

#### *In situ* UV irradiation and annealing of the matrices

The Ar and Xe matrices containing either TS or CS were submitted to *in situ* broadband irradiation in the UV ( $\lambda > 225 \text{ nm}$ ). TS was found to be photostable under these experimental conditions. On the other hand, not unexpectedly [53], CS was found to convert into TS. Upon 90 min of irradiation of CS in both argon and xenon matrices,  $\sim 70\%$  of the compound was consumed.

One of the main advantages of the matrix isolation technique is that, because of its high spectral resolution and the very small frequency shifts caused by the matrix media (taking as reference those of the molecule in gas phase), it is as a very powerful tool to detect subtle structural changes, guided by results of calculated spectra for the studied molecule *in vacuo*. A first look to the spectra of the irradiated CS matrices immediately allows to conclude that, as reported first by Kar et al. [53], in addition to the decreasing IR peaks due to reactant (CS) and the growing ones matching the IR spectrum of TS discussed in the previous section, additional new features can be observed which cannot be assigned to either of these species.<sup>1</sup>

<sup>1</sup> As discussed in detail later on, the most intense bands of this set of new bands do in fact correspond to very low intensity bands observable in the spectra of as-deposited TS. Interpretation for this will be given in another section of this article.

**Table 2**  
Observed (argon matrix; 15 K; xenon matrix; 15 K) and calculated (B3LYP/6-311++G(d,p)) IR spectra and potential energy distribution of the normal modes (PED,%) for *cis*-stilbene (C<sub>2</sub>).<sup>a</sup>

Approximate description	PED	Symmetry	Calculated		Observed (Ar) <sup>b</sup>				Observed (Xe) <sup>b</sup>			
			$\nu$	I	$\nu$	I	$\nu^{gc}$	I <sup>gc</sup>	$\nu$	I	$\nu^{gc}$	I <sup>gc</sup>
$\nu(\text{CH})_{1a}$	S <sub>2</sub> [57] + S <sub>4</sub> [41]	A	3125.8	4.6	} 3100.9	1.0	3100.9	1.0	} 3106.7	0.9	3106.7	0.9
$\nu(\text{CH})_{1b}$	S <sub>38</sub> [60] + S <sub>40</sub> [38]	B	3125.2	4.2								
$\nu(\text{CH})_{3a}$	S <sub>4</sub> [39] + S <sub>2</sub> [33] + S <sub>6</sub> [22]	A	3116.7	3.8	} 3088.5	3.6	3088.5	3.6	} 3082.0	3.4	3082.0	3.4
$\nu(\text{CH})_{3b}$	S <sub>40</sub> [41] + S <sub>38</sub> [30] + S <sub>42</sub> [22]	B	3116.4	48.7								
$\nu(\text{CH})_{5a}$	S <sub>6</sub> [45] + S <sub>5</sub> [45]	A	3105.0	26.9	} 3066.0	3.3	3066.0	3.3	} 3058.8	4.3	3058.8	4.3
$\nu(\text{CH})_{5b}$	S <sub>42</sub> [46] + S <sub>39</sub> [44]	B	3104.9	15.8								
$\nu(\text{CH})_{2a}$	S <sub>3</sub> [44] + S <sub>5</sub> [29] + S <sub>4</sub> [14]	A	3095.3	1.2	} 3055.4	2.6	3055.4	2.6	} 3053.7	3.0	3053.7	3.0
$\nu(\text{CH})_{2b}$	S <sub>39</sub> [44] + S <sub>42</sub> [28] + S <sub>40</sub> [15]	B	3095.1	0.1								
$\nu(\text{CH})_{4a}$	S <sub>5</sub> [82] + S <sub>3</sub> [11]	A	3087.5	9.2	} 3031.4	5.9	3029.2	10.2	} 3025.5	4.8	3019.7	8.3
$\nu(\text{CH})_{4b}$	S <sub>41</sub> [83] + S <sub>39</sub> [11]	B	3087.4	2.1								
$\nu_s(\text{=CH})$	S <sub>7</sub> [99]	A	3068.4	22.4							3011.8	3.5
$\nu_{as}(\text{=CH})$	S <sub>43</sub> [100]	B	3047.5	0.1							n.obs.	
$\nu(\text{C=C})$	S <sub>1</sub> [65] + S <sub>14</sub> [33] + S <sub>24</sub> [11]	A	1639.4	1.0							n.obs.	
$\nu(\text{CC})_{3b}$	S <sub>46</sub> [66] + S <sub>53</sub> [21]	B	1604.2	8.4			1604.8	7.5	1604.8	7.5	1602.8	3.1
$\nu(\text{CC})_{3a}$	S <sub>10</sub> [66] + S <sub>17</sub> [21] + S <sub>22</sub> [10]	A	1601.0	0.1			n.obs.				n.obs.	
$\nu(\text{CC})_{4b}$	S <sub>47</sub> [67] + S <sub>52</sub> [17]	B	1577.5	1.7			1580.6	1.3	1580.6	1.3	1578.9	1.2
$\nu(\text{CC})_{4a}$	S <sub>11</sub> [64] + S <sub>16</sub> [18]	A	1574.6	0.01			n.obs.				n.obs.	
$\delta(\text{CH})_{4b}$	S <sub>54</sub> [58] + S <sub>49</sub> [33]	B	1492.9	9.7			1505.6	1.6	1500.2	12.5	1501.5	2.1
							1503.5	1.6			1497.7	7.7
							1500.9	2.0			1496.3	5.6
							1498.1	7.3				
$\delta(\text{CH})_{4a}$	S <sub>18</sub> [60] + S <sub>13</sub> [32]	A	1488.2	5.2			1493.1	8.5	1493.1	8.5	1491.0	6.6
$\delta(\text{CH})_{5b}$	S <sub>48</sub> [24] + S <sub>55</sub> [23] + S <sub>52</sub> [14] + S <sub>60</sub> [13] + S <sub>51</sub> [12]	B	1447.6	9.3			1453.6	5.2	1452.4	12.1	1449.6	6.9
							1451.5	6.9			1449.6	6.9
$\delta(\text{CH})_{5a}$	S <sub>19</sub> [26] + S <sub>12</sub> [21] + S <sub>15</sub> [17] + S <sub>16</sub> [12] + S <sub>9</sub> [11]	A	1440.8	6.9			1446.7	9.8	1446.7	9.8	1444.6	9.1
$\delta_{as}(\text{=CH})$	S <sub>60</sub> [65]	B	1408.3	8.9			1411.2	1.6	1408.9	4.6	1408.9	1.2
							1408.6	1.6			1407.7	2.2
							1406.3	1.3			1406.2	1.0
$\delta(\text{CH})_{1a}$	S <sub>15</sub> [73] + S <sub>24</sub> [10]	A	1329.5	1.0			1336.9	0.6	1336.9	0.6	1334.5	0.5
$\delta(\text{CH})_{1b}$	S <sub>51</sub> [72] + S <sub>45</sub> [22]	B	1324.5	0.7			1324.8	0.5	1324.8	0.5	1320.2	0.3
$\nu(\text{CC})_{2a}$	S <sub>9</sub> [64] + S <sub>24</sub> [21]	A	1314.7	0.6			1316.1	0.5	1316.1	0.5	1315.3	0.4
$\nu(\text{CC})_{2b}$	S <sub>45</sub> [51] + S <sub>48</sub> [19]	B	1292.2	0.1			n.obs.				n.obs.	
$\delta_s(\text{=CH})$	S <sub>24</sub> [44] + S <sub>12</sub> [14] + S <sub>9</sub> [10]	A	1237.1	0.1			n.obs.				1237.6	0.3
$\nu_{as}(\text{C=C})$	S <sub>50</sub> [32] + S <sub>60</sub> [15] + S <sub>44</sub> [13] + S <sub>54</sub> [13] + S <sub>57</sub> [11]	B	1198.5	0.2			1204.9	0.3	1204.9	0.3	1204.0	0.2
$\delta(\text{CH})_{3a}$	S <sub>17</sub> [75] + S <sub>10</sub> [25]	A	1177.9	1.0			1183.4	0.9	1183.4	0.9	1181.4	1.0
$\delta(\text{CH})_{3b}$	S <sub>53</sub> [76] + S <sub>46</sub> [23]	B	1176.4	1.3			1179.8	0.9	1179.8	0.9	1178.1	0.6
$\delta(\text{CH})_{2a}$	S <sub>16</sub> [41] + S <sub>19</sub> [38] + S <sub>9</sub> [11]	A	1156.1	0.001			n.obs.				n.obs.	
$\delta(\text{CH})_{2b}$	S <sub>52</sub> [41] + S <sub>55</sub> [39] + S <sub>45</sub> [12]	B	1155.0	0.002			n.obs.				1155.5	0.7
$\nu_s(\text{C=C})$	S <sub>14</sub> [20] + S <sub>21</sub> [16] + S <sub>8</sub> [14] + S <sub>1</sub> [12] + S <sub>18</sub> [12]	A	1145.7	0.03			n.obs.				n.obs.	
$\nu(\text{CC})_{5b}$	S <sub>48</sub> [42] + S <sub>55</sub> [24] + S <sub>52</sub> [18]	B	1080.4	10.0			1077.0	3.9	1076.4	5.9	1075.0	3.3
							1075.1	2.0			1074.1	5.8
							1075.1	2.0			1072.9	2.5
$\nu(\text{CC})_{5a}$	S <sub>12</sub> [51] + S <sub>19</sub> [24] + S <sub>16</sub> [16]	A	1076.5	2.2			1073.2	1.3	1073.2	1.3	1070.5	1.5
$\nu(\text{CC})_{6b}$	S <sub>49</sub> [51] + S <sub>54</sub> [22] + S <sub>44</sub> [18]	B	1025.7	5.8			1028.6	4.9	1028.6	4.9	1029.2	1.5
$\nu(\text{CC})_{6a}$	S <sub>13</sub> [47] + S <sub>8</sub> [20] + S <sub>18</sub> [20] + S <sub>21</sub> [12]	A	1025.2	2.5			1030.6	2.6	1030.6	2.6	1032.0	4.2
$\delta(\text{Ph})_{1b}$	S <sub>57</sub> [61] + S <sub>44</sub> [38]	B	993.0	0.2			} 1011.9	0.3	1011.9	0.3	} 1001.4	0.2
$\delta(\text{Ph})_{1a}$	S <sub>21</sub> [57] + S <sub>8</sub> [42]	A	992.6	0.1								
$\gamma(\text{CH})_{5a}$	S <sub>32</sub> [63] + S <sub>30</sub> [59]	A	982.0	0.4			n.obs.				n.obs.	
$\gamma(\text{CH})_{5b}$	S <sub>66</sub> [100]	B	978.9	1.1			981.7	0.7	981.7	0.7	979.5	1.0
$\gamma_s(\text{=CH})$	S <sub>32</sub> [57] + S <sub>30</sub> [54]	A	976.2	0.5			n.obs.				n.obs.	
$\gamma(\text{CH})_{4a}$	S <sub>29</sub> [100]	A	964.7	0.01			n.obs.				n.obs.	
$\gamma(\text{CH})_{4b}$	S <sub>65</sub> [100]	B	964.6	0.6			966.4	0.5	966.4	0.5	963.6	0.7
											962.4	1.4
											961.1	0.7
$\gamma(\text{CH})_{2b}$	S <sub>63</sub> [74] + S <sub>67</sub> [11]	B	922.5	20.5			925.1	8.9	924.2	23.9	923.7	9.4
							924.1	7.5			922.8	20.8
							923.1	7.5			922.3	11.1
							923.1	7.5			911.3	0.3
$\gamma(\text{CH})_{2a}$	S <sub>27</sub> [90]	A	910.7	0.2			n.obs.				911.3	0.6
$\nu(\text{CC})_{1b}$	S <sub>61</sub> [24] + S <sub>63</sub> [19] + S <sub>44</sub> [14]	B	855.4	8.0			864.4	2.9	864.4	2.9	862.5	2.7
$\gamma(\text{CH})_{3a}$	S <sub>28</sub> [100]	A	836.5	0.1			n.obs.				n.obs.	
$\gamma(\text{CH})_{3b}$	S <sub>64</sub> [100]	B	835.5	0.4			n.obs.				839.2	0.5
$\gamma_{as}(\text{=CH})$	S <sub>68</sub> [37] + S <sub>62</sub> [15] + S <sub>67</sub> [11]	B	782.0	60.3			786.1	15.1	783.0	62.4	787.6	6.5
							784.7	11.5			781.6	67.3
							783.5	11.5			785.6	10.3
							782.6	11.5			782.3	13.4
							777.9	12.8			781.0	14.4
											779.0	14.4
											776.7	8.3
$\gamma(\text{CH})_{1a}$	S <sub>26</sub> [27] + S <sub>34</sub> [22] + S <sub>31</sub> [16]	A	767.8	5.7			772.5	5.6	771.9	13.5	769.8	4.9
							771.4	7.9			769.8	4.9
$\nu(\text{CC})_{1a}$	S <sub>22</sub> [21] + S <sub>14</sub> [18] + S <sub>26</sub> [15]	A	748.2	2.1			752.7	4.3	752.7	4.3	751.6	3.3
											751.1	5.6
											750.4	2.3
$\delta_{as}(\text{C=C=C})$	S <sub>68</sub> [32] + S <sub>61</sub> [15]	B	729.6	6.5			734.6	1.0	731.9	5.3	731.7	2.2
											730.4	6.2

(continued on next page)

					731.3	4.3			730.5	2.3		
									728.7	1.7		
$\gamma(\text{CH})_{1b}$	$S_{62}[60] + S_{69}[34]$	B	692.5	83.1	701.7	13.0	698.5	87.4	697.6	38.8	696.6	106.2
					699.0	25.6			696.9	39.7		
					697.3	48.8			694.5	26.7		
$\tau(\text{Ph})_{1a}$	$S_{34}[68] + S_{26}[44]$	A	691.6	16.4	695.1	17.2	695.1	17.2	693.0	12.3	693.0	12.3
$\tau(\text{Ph})_{1b}$	$S_{69}[67] + S_{61}[14] + S_{68}[10]$	B	681.7	0.8	684.9	2.2	684.9	2.2	683.7	3.1	683.3	4.7
									682.4	1.6		
$\delta(\text{Ph})_{3a}$	$S_{23}[85]$	A	620.2	0.01	n.obs.				n.obs.			
$\delta(\text{Ph})_{3b}$	$S_{59}[87]$	A	619.3	0.4	618.9	0.3	618.9	0.3	618.8	0.9	618.8	0.9
$\tau(\text{C}=\text{C})$	$S_{33}[53] + S_{34}[19] + S_{31}[17]$	A	564.1	3.7	561.4	2.6	561.4	2.6	560.0	2.9	559.3	4.4
									557.9	1.5		
$\delta(\text{Ph})_{2a}$	$S_{22}[47] + S_{20}[11]$	A	516.4	1.5	519.4	1.8	519.4	1.8	518.1	0.9	518.1	0.9
$\delta(\text{Ph})_{2b}$	$S_{58}[52] + S_{50}[14]$	B	501.6	13.6	502.6	3.3	501.1	6.6	504.7	2.1	501.10	7.7
					499.5	3.3			500.9	3.3		
									497.9	2.3		
$\tau(\text{Ph})_{3b}$	$S_{71}[40] + S_{67}[23] + S_{70}[16]$	B	446.1	10.1	449.4	3.3	449.4	3.3	447.4	2.1	445.3	8.6
									446.5	2.5		
									444.8	1.9		
									442.0	2.1		
$\tau(\text{Ph})_{2a}$	$S_{35}[93] + S_{36}[19]$	A	405.7	0.1								
$\tau(\text{Ph})_{3a}$	$S_{36}[42] + S_{33}[25]$	A	402.5	0.2								
$\tau(\text{Ph})_{2b}$	$S_{70}[83] + S_{71}[15]$	B	402.3	0.5								
$\delta_s(\text{C}=\text{C})$	$S_{20}[25] + S_{36}[23] + S_{25}[18] + S_{33}[11]$	A	257.0	0.5								
$w_{as}(\text{Ph}-\text{C})$	$S_{56}[51] + S_{71}[17] + S_{67}[10]$	B	244.6	2.5								
$w_s(\text{Ph}-\text{C})$	$S_{37}[59] + S_{20}[25] + S_{25}[10]$	A	156.2	0.04								
$\gamma_{as}(\text{Ph}-\text{C})$	$S_{67}[32] + S_{71}[20] + S_{66}[17] + S_{61}[14]$	B	153.7	0.8								
$\gamma_s(\text{Ph}-\text{C})$	$S_{31}[43] + S_{33}[25] + S_{25}[17]$	A	74.7	0.05								
$\tau_{as}(\text{C}-\text{C})$	$S_{72}[100]$	B	31.6	0.01								
$\tau_s(\text{C}-\text{C})$	$S_{37}[46] + S_{25}[39] + S_{20}[12]$	A	29.2	0.001								

<sup>a</sup> See Table S1 (Supporting Information) for definition of symmetry coordinates;  $\nu$ , stretching;  $\delta$ , in-plane bending;  $w$ , wagging;  $\gamma$ , out-of-plane bending;  $\tau$ , torsion;  $s$ , symmetric;  $as$ , asymmetric; Ph, phenyl; n.obs., not observed; calculated wavenumbers ( $\text{cm}^{-1}$ ) were scaled by 0.978; calculated infrared intensities in  $\text{km mol}^{-1}$ ; PED's smaller than 10% are not given;

<sup>b</sup> Observed absorbances were normalized so that the total infrared intensity of the experimental bands (excluding those of the CH stretching bands) equals the corresponding calculated intensity (for experimental CH stretchings intensities, the same normalizing factor obtained was applied); the gravity centre (gc) of a given band was calculated as the intensity averaged mean wavenumber for the band components ascribed to a given vibration.

These new bands could be easily evidenced upon annealing of the irradiated matrices to higher temperatures, since they reduce intensity till disappearance in favor of the features due to TS.

Figs. 3 and 4 show the difference spectra (in argon and in xenon matrices, respectively) resulting from subtracting to the spectra obtained immediately after irradiation of the matrices the spectra after annealing of the irradiated matrices. As shown in Figs. 3 and 4, the species produced after irradiation that convert into TS upon annealing of the matrices has an IR spectrum compatible with the suggestion of Kar et al. [53], which assigned it to a non-planar form of TS. In order to characterize structurally in more detail this non-planar TS form, the IR spectrum of TS was calculated (at the B3LYP/6-311++G(d,p)) as a function of the lowest energy C–phenyl symmetric torsional vibration [ $\tau_s(\text{C}-\text{C})$ ]. In TS-type structures, this vibration corresponds to a well-localized vibration (see Table 1) so that calculation of the vibrational spectrum for different values of the torsional coordinate are meaningful (forces along other coordinates are null for a full relaxed structure along the torsional coordinate). Non-planar structures where only one of the phenyl groups were moved out of the molecular plane were also considered in these calculations. The calculated spectra were then compared with the observed ones using standard chemometric methods, as described in detail in the next section. Among all the investigated structures, the one where the two phenyl groups are placed out of the plane of the ethylene moiety by  $30^\circ$  (designated here as 30–30) gives the best fits to the experimental data. In Figs. 3 and 4, the calculated spectrum of this non-planar TS form is compared with the experimental results. A simulated difference spectrum (non-planar TS minus planar TS) is also shown in these figures to make the comparison between the experimental and calculated spectra easier. As it can be seen, the reproduction by the theoretical calculations of the experimentally observed spectrum of the non-planar TS form is excellent. Table 3 shows the complete

assignment of the spectra of the non-planar TS in both argon and xenon matrices.

#### Chemometrics similarity analyses for identification of the non-planar TS form

The determination of the most probable geometry of the non-planar TS form experimentally observed upon UV-induced isomerization of matrix-isolated CS was based in a series of comparisons between the calculated spectra for different non-planar configurations of the molecule and the experimental spectra. As references, either the spectra of CS and planar TS were used.

A first, simpler comparison was made by calculating the distances ( $d$ ) between vectors built from absolute wavenumbers ( $\nu$ ), absolute intensities ( $I$ ) and wavenumber shifts in relation to the reference CS or planar TS structure for all vibrations whose experimental bands allowed reliable wavenumber and intensity determinations:

$$d_\alpha = \sum \left\{ \sqrt{(\nu_{\text{cal}} - \nu_{\text{exp}})^2 + (I_{\text{cal}} - I_{\text{exp}})^2 + [(\nu_\alpha - \nu_{\text{cal}}) - (\nu_\alpha - \nu_{\text{exp}})]^2} \right\}, \quad (1)$$

where  $\alpha$  = CS or planar TS

The results are shown in Table 4, where it can be seen that among all structures considered the one where the two phenyl groups are placed out of the plane of the ethylene moiety by  $30^\circ$  (of  $C_2$  symmetry, according to the deformations corresponding to the lowest energy vibration,  $\tau_s(\text{C}-\text{C})$ ) gives the best fits to the experimental data, both when the reference structure is CS or planar TS.

The same information was then used in a principal component analysis. The obtained results are depicted in Figs. 5 and 6, where graphs of PC2 vs. PC1 are shown to reveal the proximity of the different structures in relation to the chosen reference structure

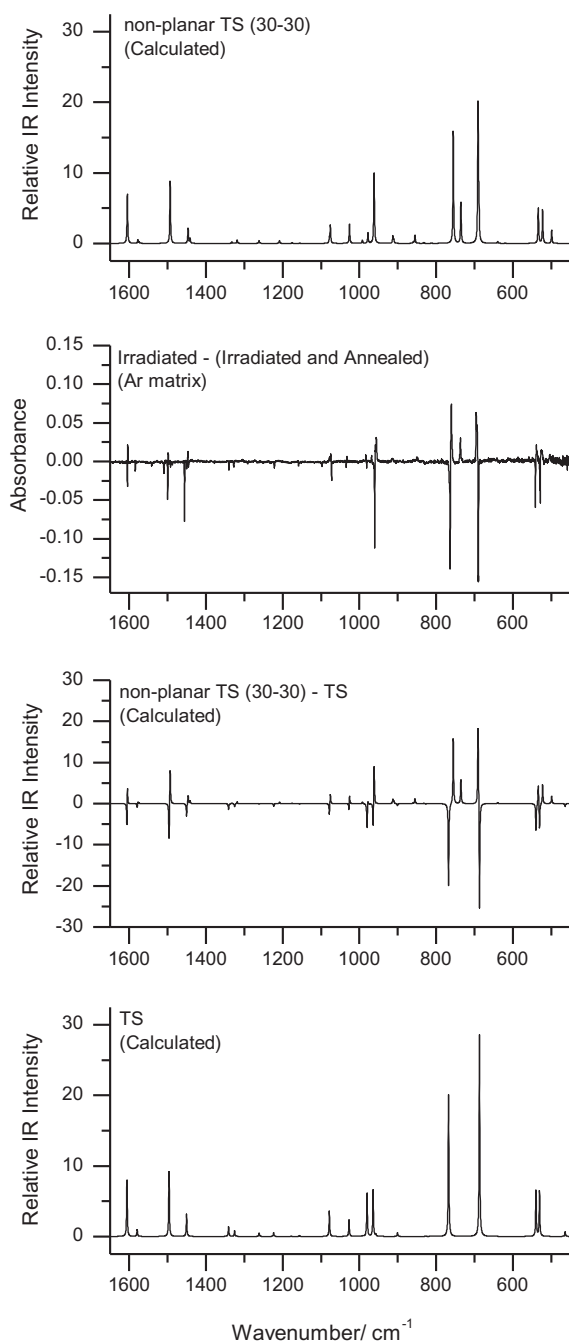


**Fig. 3.** From top to bottom: B3LYP/6-311++G(d,p) calculated infrared spectrum (1650–450  $\text{cm}^{-1}$  range) of non-planar *trans*-stilbene (30–30 conformation); infrared difference spectrum (spectrum of the irradiated matrix *minus* spectrum of the irradiated and annealed matrix) obtained in argon; simulated non-planar TS *minus* planar TS difference IR spectrum; calculated infrared spectrum of *trans*-stilbene. In the calculated spectra, wavenumbers were scaled by 0.978; the bands were simulated using Lorentzian functions with full widths at half-maximum-height (fwhm) of 2  $\text{cm}^{-1}$  centered at the scaled wavenumbers.

(CS or planar-TS) in what concerns to wavenumbers, intensities, wavenumber shifts (Fig. 6), or to all these descriptors simultaneously (Fig. 5). In all cases the 30–30 structure appears as the nearest non-planar TS structure compared to the reference experimental data. Very interestingly, in all graphs it is clear that among those structures with equal values of the two dihedral angles about the C–Phenyl bonds (i.e., the structures appearing along the lowest energy  $\tau_s(\text{C–C})$  vibration; connected by the lines

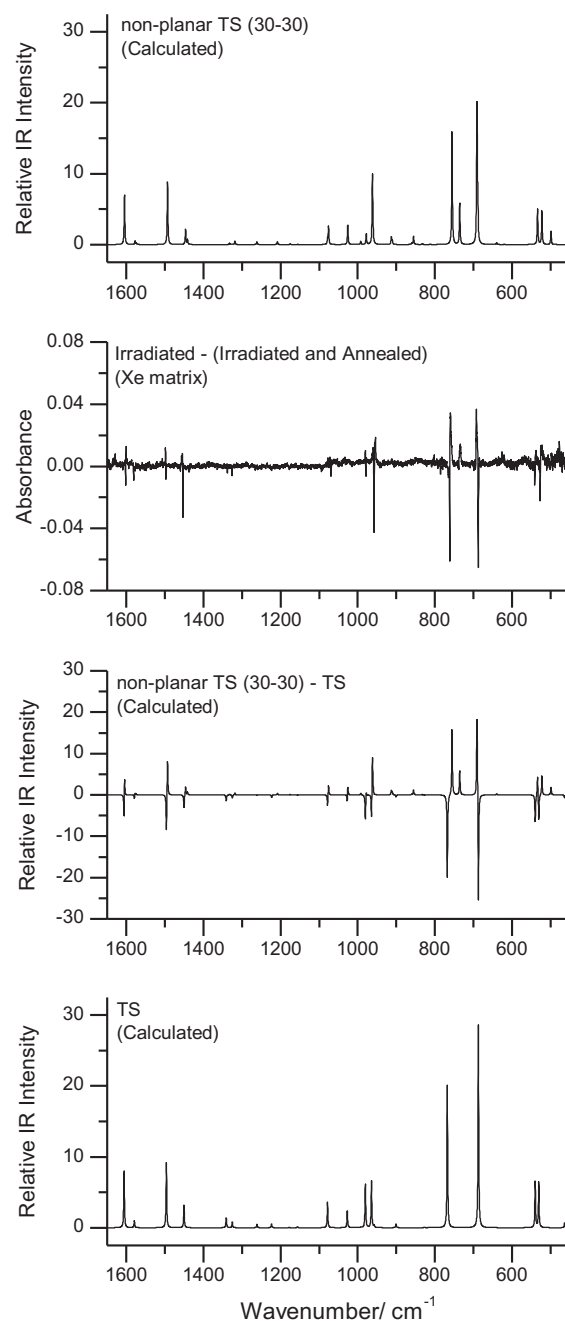


**Fig. 4.** From top to bottom: B3LYP/6-311++G(d,p) calculated infrared spectrum (1650–450  $\text{cm}^{-1}$  range) of nonplanar *trans*-stilbene (30–30 conformation); infrared difference spectrum (spectrum of the irradiated matrix *minus* spectrum of the irradiated and annealed matrix) obtained in xenon; simulated non-planar TS *minus* planar TS difference IR spectrum; calculated infrared spectrum of *trans*-stilbene. In the calculated spectra, wavenumbers were scaled by 0.978; the bands were simulated using Lorentzian functions with full widths at half-maximum-height (fwhm) of 2  $\text{cm}^{-1}$  centered at the scaled wavenumbers.

in Figs. 5 and 6), those where the dihedral angles are smaller than 30° and those where the dihedrals are larger than 30° diverge towards different directions in the plots from the position of the best 30–30 structure. This is a clear indication of the singular nature of the 30–30 structure in relation to the observed non-planar TS species from a similarity point of view, and can be considered an additional piece of information sustaining the assignment of the 30–30 structure to the experimentally observed one.

**Table 3**Observed (argon matrix; 15 K; xenon matrix; 15 K) and calculated (B3LYP/6-311++G(d,p)) IR spectra and potential energy distribution of the normal modes (PED,%) for *trans*-stilbene (non-planar; C<sub>2</sub>).<sup>a</sup>

Approximate description	PED	Symmetry	Calculated		Observed (Ar) <sup>b</sup>		Observed (Xe) <sup>b</sup>	
			$\nu$	I	$\nu$	I	$\nu$	I
$\nu(\text{CH})_{1a}$	S <sub>2</sub> [86]	A	3119.8	0.04	n.obs.		n.obs.	
$\nu(\text{CH})_{1b}$	S <sub>38</sub> [85]	B	3119.6	38.0	3117.4	2.3	n.obs.	
$\nu(\text{CH})_{3b}$	S <sub>40</sub> [70] + S <sub>39</sub> [24]	B	3110.2	41.7	3092.3	4.3	3086.4	10.2
$\nu(\text{CH})_{3a}$	S <sub>4</sub> [69] + S <sub>3</sub> [23]	A	3110.1	13.1				
$\nu(\text{CH})_{5a}$	S <sub>6</sub> [78] + S <sub>3</sub> [12]	A	3103.3	1.3	n.obs.		n.obs.	
$\nu(\text{CH})_{5b}$	S <sub>42</sub> [78] + S <sub>39</sub> [11] + S <sub>38</sub> [10]	B	3103.1	16.7	3081.7	4.9	3065.1	16.9
$\nu(\text{CH})_{2b}$	S <sub>39</sub> [46] + S <sub>20</sub> [28] + S <sub>41</sub> [18]	B	3093.6	0.2	n.obs.		n.obs.	
$\nu(\text{CH})_{2a}$	S <sub>3</sub> [48] + S <sub>4</sub> [30] + S <sub>5</sub> [16]	A	3093.4	0.01	n.obs.		n.obs.	
$\nu(\text{CH})_{4a}$	S <sub>5</sub> [76] + S <sub>3</sub> [16]	A	3088.1	0.2	n.obs.		n.obs.	
$\nu(\text{CH})_{4b}$	S <sub>41</sub> [73] + S <sub>39</sub> [19]	B	3088.0	15.0	3041.4	5.6	3033.4	18.1
$\nu_{as}(\text{=CH})$	S <sub>43</sub> [98]	B	3069.3	27.9	3029.2	3.7	3018.5	11.3
$\nu_s(\text{=CH})$	S <sub>7</sub> [99]	A	3061.5	0.1	n.obs.		n.obs.	
$\nu(\text{C=C})$	S <sub>1</sub> [59] + S <sub>24</sub> [20]	A	1644.5	0.02	n.obs.		n.obs.	
$\nu(\text{CC})_{3b}$	S <sub>46</sub> [66] + S <sub>53</sub> [21] + S <sub>58</sub> [10]	B	1605.0	22.0	1604.0	15.0	1601.0	16.8
$\nu(\text{CC})_{3a}$	S <sub>10</sub> [65] + S <sub>17</sub> [21] + S <sub>22</sub> [10]	A	1599.7	0.0	n.obs.		n.obs.	
$\nu(\text{CC})_{4b}$	S <sub>47</sub> [67] + S <sub>52</sub> [17]	B	1577.6	1.7	1581.5	1.4	1576.2	3.0
$\nu(\text{CC})_{4a}$	S <sub>11</sub> [64] + S <sub>16</sub> [18]	A	1574.4	0.5	n.obs.		n.obs.	
$\delta(\text{CH})_{4b}$	S <sub>54</sub> [59] + S <sub>49</sub> [33]	B	1493.4	28.1	1498.6	14.7	1498.8	15.6
$\delta(\text{CH})_{4a}$	S <sub>18</sub> [62] + S <sub>13</sub> [33]	A	1487.1	0.05	n.obs.		n.obs.	
$\delta(\text{CH})_{5b}$	S <sub>48</sub> [26] + S <sub>55</sub> [24] + S <sub>52</sub> [15] + S <sub>51</sub> [14]	B	1446.6	6.8	1447.0	10.1	1455.7	11.0
$\delta(\text{CH})_{5a}$	S <sub>19</sub> [26] + S <sub>12</sub> [22] + S <sub>15</sub> [17] + S <sub>16</sub> [12] + S <sub>9</sub> [11]	A	1441.6	2.1	1436.7	2.6	n.obs.	
$\delta(\text{CH})_{1b}$	S <sub>51</sub> [63] + S <sub>60</sub> [24]	B	1332.5	0.5	n.obs.		n.obs.	
$\delta(\text{CH})_{1a}$	S <sub>15</sub> [71] + S <sub>9</sub> [19]	A	1325.9	0.2	n.obs.		n.obs.	
$\nu(\text{CC})_{2b}$	S <sub>45</sub> [70] + S <sub>51</sub> [12] + S <sub>60</sub> [12]	B	1318.7	1.5	1306.0	2.5	n.obs.	
$\delta_s(\text{=CH})$	S <sub>24</sub> [50] + S <sub>9</sub> [28] + S <sub>1</sub> [15]	A	1310.5	0.01	n.obs.		n.obs.	
$\nu(\text{CC})_{2a}$	S <sub>9</sub> [29] + S <sub>24</sub> [16] + S <sub>12</sub> [16] + S <sub>25</sub> [11]	A	1294.4	0.001	n.obs.		n.obs.	
$\nu_{as}(\text{C-C})$	S <sub>50</sub> [37] + S <sub>54</sub> [10]	B	1261.6	1.2	1272.4	2.0	1275.3	2.2
$\delta_{as}(\text{=CH})$	S <sub>60</sub> [47] + S <sub>50</sub> [11]	B	1208.4	1.2	n.obs.		n.obs.	
$\nu_s(\text{C-C})$	S <sub>14</sub> [27] + S <sub>8</sub> [13] + S <sub>21</sub> [12] + S <sub>18</sub> [11]	A	1186.5	0.003	n.obs.		n.obs.	
$\delta(\text{CH})_{3b}$	S <sub>53</sub> [76] + S <sub>46</sub> [22]	B	1175.4	0.2	n.obs.		n.obs.	
$\delta(\text{CH})_{3a}$	S <sub>17</sub> [72] + S <sub>10</sub> [20]	A	1175.1	0.1	n.obs.		n.obs.	
$\delta(\text{CH})_{2a}$	S <sub>16</sub> [43] + S <sub>19</sub> [38] + S <sub>9</sub> [11]	A	1155.6	0.0	n.obs.		n.obs.	
$\delta(\text{CH})_{2b}$	S <sub>52</sub> [41] + S <sub>55</sub> [40] + S <sub>45</sub> [11]	B	1155.5	0.1	1141.4	0.9	n.obs.	
$\nu(\text{CC})_{5a}$	S <sub>12</sub> [46] + S <sub>19</sub> [24] + S <sub>16</sub> [16]	A	1078.4	2.2	1078.3	4.9	1072.7	5.2
$\nu(\text{CC})_{5b}$	S <sub>48</sub> [53] + S <sub>55</sub> [22] + S <sub>52</sub> [16]	B	1075.7	7.9	1074.6	7.9	1067.3	5.5
$\nu(\text{CC})_{6b}$	S <sub>49</sub> [52] + S <sub>54</sub> [23] + S <sub>44</sub> [18]	B	1025.8	8.6	1032.6	5.7	1032.6	7.7
$\nu(\text{CC})_{6a}$	S <sub>13</sub> [50] + S <sub>18</sub> [22] + S <sub>8</sub> [19]	A	1024.9	0.05	n.obs.		n.obs.	
$\delta(\text{Ph})_{1a}$	S <sub>21</sub> [59] + S <sub>8</sub> [37]	A	992.2	1.3	983.2	6.8	980.1	13.6
$\delta(\text{Ph})_{1b}$	S <sub>57</sub> [64] + S <sub>44</sub> [35]	B	992.2	0.05	n.obs.		n.obs.	
$\gamma(\text{CH})_{5a}$	S <sub>30</sub> [100]	A	977.9	4.7	968.3	6.3	962.1	11.5
$\gamma(\text{CH})_{5b}$	S <sub>66</sub> [100]	B	975.8	0.02	n.obs.		n.obs.	
$\gamma_s(\text{=CH})$	S <sub>32</sub> [81] + S <sub>29</sub> [13]	A	961.8	29.7	955.2	23.7	954.2	24.4
$\gamma(\text{CH})_{4a}$	S <sub>29</sub> [100]	A	960.5	3.8	n.obs.		n.obs.	
$\gamma(\text{CH})_{4b}$	S <sub>65</sub> [100]	B	960.4	0.05	n.obs.		n.obs.	
$\gamma(\text{CH})_{2b}$	S <sub>63</sub> [74] + S <sub>68</sub> [15] + S <sub>67</sub> [11]	B	912.8	3.3	913.4	3.4	912.2	6.2
$\gamma(\text{CH})_{2a}$	S <sub>27</sub> [76]	A	910.5	1.7	n.obs.		n.obs.	
$\nu(\text{CC})_{1a}$	S <sub>25</sub> [25] + S <sub>8</sub> [17] + S <sub>27</sub> [14] + S <sub>14</sub> [10] + S <sub>21</sub> [10]	A	859.8	0.6	860.0	2.4	862.0	1.3
$\gamma_{as}(\text{=CH})$	S <sub>68</sub> [68] + S <sub>63</sub> [21]	B	855.1	3.7	848.2	4.0	840.5	3.9
$\gamma(\text{CH})_{3a}$	S <sub>28</sub> [99]	A	832.2	0.2	n.obs.		n.obs.	
$\gamma(\text{CH})_{3b}$	S <sub>64</sub> [94]	B	831.8	0.1	n.obs.		n.obs.	
$\nu(\text{CC})_{1b}$	S <sub>44</sub> [28] + S <sub>50</sub> [26] + S <sub>57</sub> [16] + S <sub>58</sub> [12]	B	811.8	0.1	n.obs.		n.obs.	
$\gamma(\text{CH})_{1a}$	S <sub>26</sub> [42] + S <sub>34</sub> [29] + S <sub>31</sub> [18]	A	755.2	50.0	760.3	55.4	759.2	45.4
$\gamma(\text{CH})_{1b}$	S <sub>62</sub> [56] + S <sub>69</sub> [25]	B	735.4	18.5	736.5	23.0	734.1	19.3
$\tau(\text{Ph})_{1a}$	S <sub>34</sub> [69] + S <sub>26</sub> [42]	A	690.6	61.6	695.5	55.3	692.8	48.5
$\tau(\text{Ph})_{1b}$	S <sub>69</sub> [84] + S <sub>62</sub> [31]	B	688.4	15.8	693.3	24.0	689.8	24.3
$\tau(\text{Ph})_{2a}$	S <sub>22</sub> [61] + S <sub>25</sub> [19]	A	639.2	0.8	n.obs.		n.obs.	
$\delta(\text{Ph})_{3b}$	S <sub>59</sub> [86]	B	621.2	0.01	n.obs.		n.obs.	
$\delta(\text{Ph})_{3a}$	S <sub>23</sub> [87]	A	619.1	0.1	n.obs.		620.3	
$\delta(\text{Ph})_{2b}$	S <sub>58</sub> [77] + S <sub>50</sub> [11]	B	533.4	15.9	538.4	16.8	537.1	13.2
$\gamma_s(\text{Ph-C})$	S <sub>31</sub> [33] + S <sub>36</sub> [22] + S <sub>33</sub> [18] + S <sub>34</sub> [16]	A	522.2	14.9	525.4	11.7	523.2	17.8
$\gamma_{as}(\text{Ph-C})$	S <sub>67</sub> [27] + S <sub>71</sub> [21] + S <sub>56</sub> [15] + S <sub>61</sub> [15]	B	498.7	5.9	501.9	7.1	497.4	7.8
$w_{as}(\text{Ph-C})$	S <sub>56</sub> [37] + S <sub>71</sub> [23] + S <sub>61</sub> [14] + S <sub>67</sub> [10]	B	421.9	1.0				
$\tau(\text{Ph})_{2b}$	S <sub>70</sub> [84] + S <sub>71</sub> [30]	B	404.8	1.3				
$\delta(\text{Ph})_{2a}$	S <sub>35</sub> [85] + S <sub>36</sub> [28]	A	404.4	0.0				
$w_s(\text{Ph-C})$	S <sub>20</sub> [37] + S <sub>36</sub> [27] + S <sub>33</sub> [19]	A	341.3	0.1				
$\tau(\text{Ph})_{3a}$	S <sub>36</sub> [23] + S <sub>14</sub> [20] + S <sub>22</sub> [14] + S <sub>25</sub> [10]	A	253.1	0.1				
$\tau(\text{Ph})_{3b}$	S <sub>71</sub> [29] + S <sub>67</sub> [27] + S <sub>72</sub> [20] + S <sub>70</sub> [15]	B	219.8	1.1				
$\delta_s(\text{C-C=C})$	S <sub>20</sub> [31] + S <sub>25</sub> [23]	A	167.9	0.1				
$\tau_{as}(\text{C-C})$	S <sub>72</sub> [77] + S <sub>56</sub> [10]	B	124.4	0.02				

(continued on next page)

**Table 3** (continued)

Approximate description	PED	Symmetry	Calculated		Observed (Ar) <sup>b</sup>		Observed (Xe) <sup>b</sup>	
			$\nu$	I	$\nu$	I	$\nu$	I
$\delta_{as}(\text{C}=\text{C})$	$S_{61}[60] + S_{56}[18] + S_{67}[11]$	B	61.7	0.2				
$\tau(\text{C}=\text{C})$	$S_{33}[58] + S_{31}[30]$	A	54.5	0.5				
$\tau_s(\text{C}-\text{C})$	$S_{37}[100]$	A	34.9	0.01				

<sup>a</sup> See Table S1 (Supporting Information) for definition of symmetry coordinates;  $\nu$ , stretching;  $\delta$ , in-plane bending;  $w$ , wagging;  $\gamma$ , out-of-plane bending;  $\tau$ , torsion;  $s$ , symmetric;  $as$ , asymmetric; Ph, phenyl;  $n.obs.$ , not observed; calculated wavenumbers ( $\text{cm}^{-1}$ ) were scaled by 0.978; calculated infrared intensities in  $\text{km mol}^{-1}$ ; PED's smaller than 10% are not given;

<sup>b</sup> Observed absorbances were normalized so that the total infrared intensity of the experimental bands (excluding those of the CH stretching bands) equals the corresponding calculated intensity (for experimental CH stretchings intensities, the same normalizing factor obtained was applied).

**Table 4**

Calculated similarity distances (according to Eq. (1)) for calculated and observed non-planar TS forms in reference to planar TS and CS.

Form <sup>a</sup>	$d_{TS}$	$d_{CS}$
5–5 220.5	306.4	
15–15	211.7	284.3
20–20	181.6	241.7
25–25	170.4	220.8
<b>30–30</b>	<b>164.2</b>	<b>204.3</b>
60–60	228.9	344.4
90–90	201.7	373.8
0–30	179.2	236.0
0–60	184.9	208.6
0–90	215.6	253.4
30–60	201.8	276.7
30–90	197.6	251.8
30–120	188.7	268.7
30–150	210.5	318.8
60–90	181.3	307.2
60–120	201.3	360.5
60–150	191.4	277.8

The bold numbers indicate data for the form (30–30) which is proposed to correspond to the non-planar observed form of *trans*-stilbene.

<sup>a</sup> The structures are designated by the values of the two dihedral angles defined around the two C–Phenyl bonds.

### 3.4. Non-planar vs. planar TS

As mentioned in the Introduction, the ground state structure of TS has been a subject of continuous discussion [33,44]. It is now accepted that in gas phase the planar geometry is the global minimum energy conformation [40,41], but evidence has also been presented that non-planar conformations may easily be stabilized by intermolecular interactions (e.g., in solutions and the pure liquid TS [50–52]). Even for the isolated molecule, these non-planar conformations were concluded to be stabilized in relation to the planar form by zero-point vibrational effects [40], so that the possibility of existence of a stable non-planar conformation with energy close to that of the planar structure and a low energy barrier separating these forms appears as a real possibility. Very unfortunately, theory has produced contradictory results [40,44] regarding this point, with the obtained data being very much dependent on the level of theory and basis sets used. Under these circumstances, experimental evidence gains additional relevance. The present investigation is a strong indication of the existence of a second (non-planar) experimentally relevant conformer of TS, even in gas phase. This conclusion can be extracted based on the following observations: (a) As shown in the previous sections, the non-planar TS form can be easily produced upon UV-photolysis of matrix-isolated CS. According to the relative intensities of bands in the matrices IR spectra collected immediately after irradiation ceased, the amount of the non-planar TS form was found to constitute about 26% of the photoproduct species. The fact that in the matrix media this non-planar form is a minimum energy

conformation is clearly shown by the observation that its conversion to the most stable planar TS form requires the temperature of the matrix to be increased (i.e., there is an energy barrier separating the two forms, which must be surpassed during the non-planar TS  $\rightarrow$  planar TS conversion). (b) On the other hand, a detailed inspection of the spectra of the as-deposited matrices of TS shows that bands due to the non-planar TS form can also be observed in those spectra, thought as a very low intensity features. Such observation requires that the non-planar TS form does exist in the gas phase prior to deposition. Note that the amount of the non-planar form in the as-deposited matrices of TS is only  $\sim 5\%$ , a value which would be compatible with a difference of energy between the non-planar and planar TS forms of ca.  $9 \text{ kJ mol}^{-1}$ . However, this energy difference shall indeed be much smaller. In fact, extensive conformational cooling during deposition of the matrices can be expected to take place in the present case, since the very low energy barrier separating the two forms can be easily overcome at the time of landing of the TS molecules (carried on the high temperature gaseous beam) onto the cold substrate of the cryostat. Conformational cooling during cryogenic matrices deposition is a common phenomenon and has been addressed in detail, for instance, in Ref. [62].

The conditions used to populate the non-planar TS form in the present experiments (*in situ* photoisomerization of matrix-isolated CS) appear to be particularly favorable for the stabilization of this species. First of all, because the isomerization reaction takes place under restricted volume conditions and, compared to planar TS, the molecular volume of the non-planar TS form (the 30–30 form, as shown above) is more similar to that of CS: the B3LYP/6-311++G(d,p) calculated spatial extents for CS, non-planar TS and planar TS are 3225, 4294 and 4327 a.u., respectively (a superposition of the calculated structures for non-planar and planar TS with CS yielded a normalized root-mean-square-deviation ratio of structures similarity of 1:0.92, favoring the non-planar TS form). Hence, rearrangement of the host matrix atoms defining the primary CS occupied matrix cages is less energetically demanding for CS  $\rightarrow$  non-planar TS than for CS  $\rightarrow$  planar TS transformation. Secondly, because the mechanism for UV isomerization of CS into TS implies mediation of the  $S_1$  minimum where the two phenyl rings are nearly perpendicular to each other [1,5,6,14–20]; hence, the ground state non-planar form can be reached firstly than the planar structure. Finally, because of the low work temperature (15 K), the probability of the non-planar form to survive the energy relaxation processes following its immediate production in a vibrationally excited state can be expected to be significant, and once vibrationally relaxed it is kept stable; as observed, a temperature increase was required to allow overcoming of the energy barrier separating this form from the most stable TS planar form.

### 3.5. Natural bond interactions and electronic effects in stilbenes

Since besides the above mentioned zero-point vibrational effects [40] electronic resonance effects can be expected to be

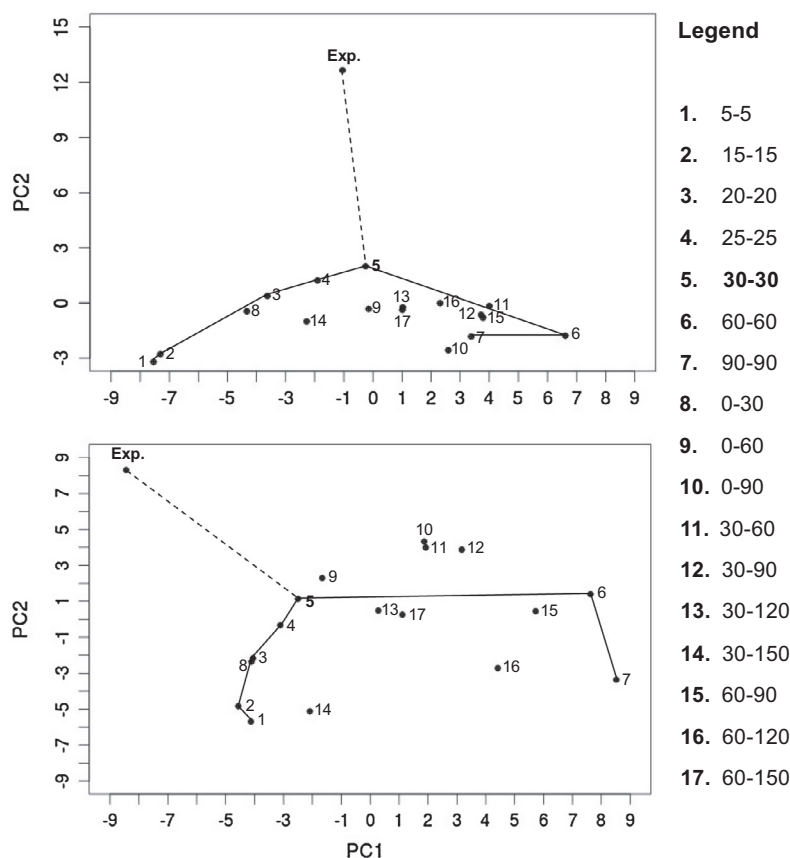


**Fig. 5.** Principal component analysis, PC2 vs. PC1 graphs, showing the relative similarities of the calculated non-planar TS structures compared to experimental data for the observed non-planar TS form, using as reference the planar TS form (*top panel*) or CS (*bottom*). Data used in the analysis were absolute wavenumbers, absolute intensities and wavenumber shifts for all vibrations whose bands allow doubtless measurement of both wavenumber position and intensity (for multiplet-like observed bands, band gravity centers were used; see [Tables 1 and 2](#)). The structures are designated in the legend of the figure by the values of the two dihedral angles defined around the two C–Phenyl bonds; those with equal values of the two dihedral angles occur along the lowest energy  $\tau_3(\text{C–C})$  coordinate and are connected by a line in the figure.

essential in determining the relative energies and properties of the different structures of stilbene, an analysis of the electronic structures of CS and both planar and non-planar conformers of TS was carried out, by examining the orbital interactions in the different molecules with help of the natural bond orbital (NBO) method [58,59]. According to the calculations, the most relevant NBO interactions for the different molecules are listed in [Table 5](#). Orbital interaction energies,  $E(2)$ , between filled (donor) and empty (acceptor) NBOs are obtained from the second-order perturbation approach [59],

$$E(2) = \Delta E_{ij} = q_i F_{ij}^2 / (\epsilon_j - \epsilon_i) \quad (2)$$

where  $F_{ij}^2$  is the Fock matrix element between the  $i$  and  $j$  NBO orbitals;  $\epsilon_j$  and  $\epsilon_i$  are the energies of the acceptor and donor NBOs; and  $q_i$  is the occupancy of the donor orbital. In [Table 5](#), NBO interactions of types A to F (together with the equivalent ones involving the second phenyl ring) are related with the mesomerism within the phenyl rings, while interactions G and H express the electron donations from the ring to the central double bond and vice versa, which describe the conjugation involving the phenyl ring and the ethylenic bond. The sums of interactions A to F amount to 503.9, 495.8 and 502.4  $\text{kJ mol}^{-1}$  (per ring) in CS, non-planar TS and TS, respectively, and show that the delocalization within the phenyl rings is, as could be anticipated, slightly more important in the bent CS and non-planar TS than in the planar TS, while, on the contrary, the conjugation between the phenyl rings and the central ethylenic bond follows the order: planar TS > non-planar TS > CS (as

expressed by the sums of G and H type NBO interactions of 117.2, 93.6 and 72.6  $\text{kJ mol}^{-1}$ , respectively; see [Table 5](#)). It is also interesting to note that the phenyl rings appear as effective charge donors to the ethylenic moiety, since in all cases the type-G NBO interaction (which transfers electron charge from the phenyl ring to the ethylenic fragment) is more important than type-H NBO interaction (which produces the opposite effect).

A simple approximate estimation of the resonance energies within the phenyl rings in the stilbene molecules and those associated with the ring/ethylenic conjugation in these molecules can also be made, assuming that the sum of the NBO interaction energies describing resonance effects in TS (shown in [Table 5](#)) are roughly proportional to the experimentally determined resonance energy for this molecule. The resonance energy for TS was determined from thermochemical data as being  $-394.6 \text{ kJ mol}^{-1}$  [63]. A scaling factor of 3.1 is then obtained as the ratio between the total NBO interaction energy for TS and the experimental resonance energy. By applying this scale factor to the remaining calculated NBO interaction energies expressing the different fractional resonance effects, the following values for the resonance energies within each phenyl ring and associated with the ring/ethylenic conjugation in CS, TS and non-planar TS can be obtained:  $-163$ ,  $-160$  and  $-162 \text{ kJ mol}^{-1}$ , and  $-23$ ,  $-38$  and  $-30 \text{ kJ mol}^{-1}$ , respectively. The first set of values are all slightly smaller than the experimental resonance energy for benzene ( $-175 \text{ kJ mol}^{-1}$  [64]), and can be explained by the competitive delocalization effect due to the conjugation between the phenyl rings and the ethylenic moiety in the stilbenes. On the other hand, the ring/ethylenic resonance

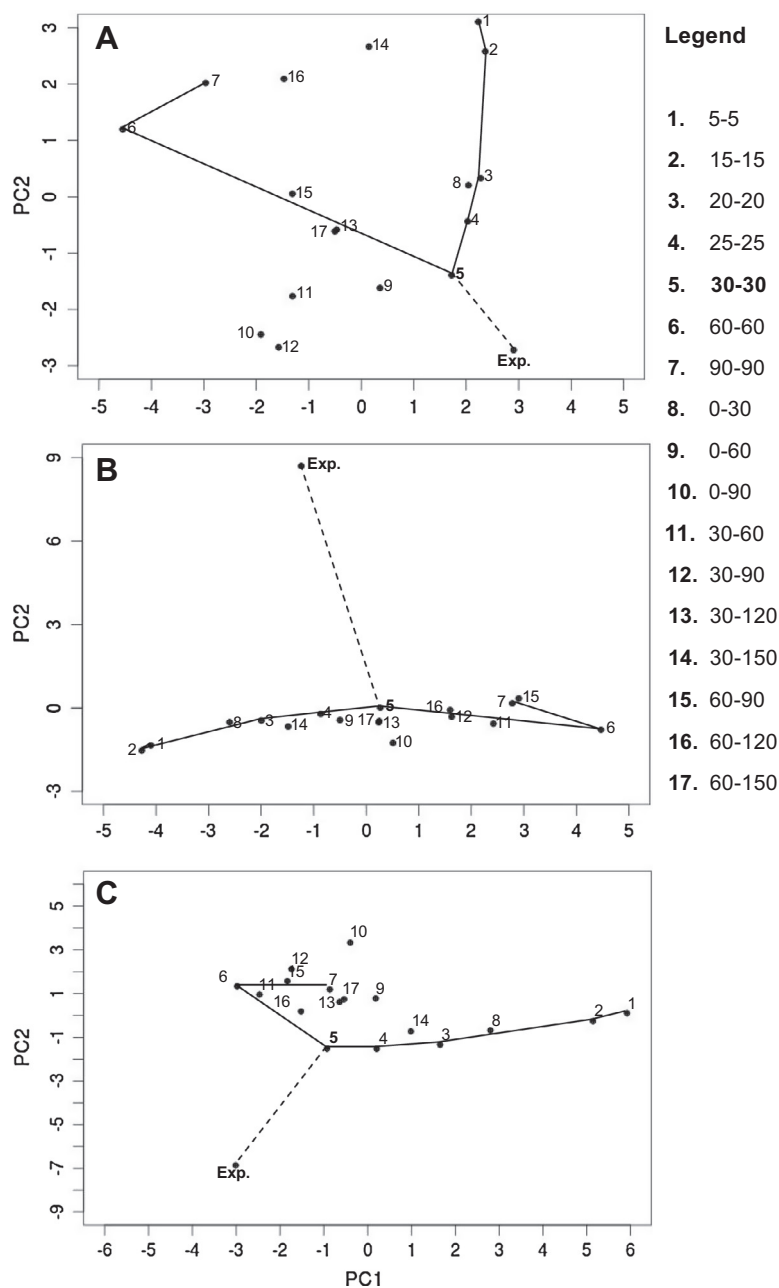


**Fig. 6.** Principal component analysis, PC2 vs. PC1 graphs, showing the relative similarities of the calculated nonplanar TS structures compared to experimental data for the observed non-planar TS form, using as reference the planar TS form. Data used in the analysis were: A – absolute intensities, B – absolute wavenumbers, and C – wavenumber shifts, for all vibrations whose bands allow doubtless measurement of both wavenumber position and intensity (for multiplet-like observed bands, band gravity centers were used; see Table 1). The structures are designated in the legend of the figure by the values of the two dihedral angles defined around the two C-Phenyl bonds; those with equal values of the two dihedral angles occur along the lowest energy  $\tau_5(\text{C}-\text{C})$  coordinate and are connected by a line in the figure.

energy is estimated by this way as being slightly smaller in CS than in butadiene ( $-27 \text{ kJ mol}^{-1}$  [64]), but somewhat larger than in this molecule in case of the TS structures (in particular for planar TS, as it could be anticipated).

#### 4. Conclusions

Monomers of *cis*- (CS) and *trans*-stilbene (TS) (planar and non-planar structures) isomers were isolated in cryogenic inert gas matrices (Ar and Xe). The identification/characterization of these species was done by IR spectroscopy and extensive theoretical calculations undertaken at the DFT(B3LYP)/6-311++G(d,p) level of

approximation. Full assignment of the infrared spectra of the stilbenes in argon and xenon matrices was undertaken.

*In situ* broadband UV irradiation of the matrix-isolated CS led to its isomerization to TS, which appeared in the photolysed matrices in both non-planar and planar configurations. The non-planar species was found to convert into the more stable planar form upon subsequent annealing of the matrices at higher temperature. The structure of the non-planar TS form was assigned based on the comparison of its observed IR spectrum with those theoretically predicted for different conformations of TS. Chemometrics was used to make this assignment. The conditions used to populate the non-planar TS form in the present experiments (*in situ* photoisomerization of cage confined CS isolated in a cryogenic inert

**Table 5**

Stabilization energies for selected NBO pairs as given by second-order perturbation theory analysis of the Fock matrix in the NBO basis for CS, TS and non-planar TS (30–30) form, obtained from the B3LYP/6-311++G(d,p) calculations. <sup>a</sup>

Pair name	Donor NBO	Acceptor NBO	$-E(2)/kJ\ mol^{-1}$		
			CS	TS	Non-planar TS (30–30)
A	$\pi(C1-C2)$	$\pi^*(C3-C4)$	87.3	87.8	88.6
B	$\pi(C1-C2)$	$\pi^*(C5-C6)$	81.5	78.8	80.0
C	$\pi(C3-C4)$	$\pi^*(C1-C2)$	84.2	83.0	83.3
D	$\pi(C3-C4)$	$\pi^*(C5-C6)$	82.4	83.1	84.2
E	$\pi(C5-C6)$	$\pi^*(C1-C2)$	83.7	81.6	83.4
F	$\pi(C5-C6)$	$\pi^*(C3-C4)$	84.8	81.3	82.6
G	$\pi(C1-C2)$	$\pi^*(C12-C14)$	40.3	63.4	49.9
H	$\pi(C12-C14)$	$\pi^*(C1-C2)$	32.3	53.8	43.7

<sup>a</sup> See atom numbering in Scheme 1. Values only presented for half of the molecule; equal stabilization energies result for the symmetrically equivalent second half of the molecule.

matrix) appeared to be particularly favorable for the stabilization and experimental characterization of this species. Observation of the non-planar TS form in the as-deposited matrices of TS allowed also concluding on the experimental relevance of this species in the gas phase.

Additional reasoning on the structure of the studied stilbenes, in particular related with electronic conjugation on CS, TS and non-planar TS, was also presented, taking as basis results of the Natural Bond Orbital analysis and available data on resonance energies for the relevant systems.

## Acknowledgements

These studies were performed under project PTDC/QUI-QUI/111879/2009 (also funded by COMPETE-QREN-EU). The authors would like also to thank Prof. A.A.C. Pais and Tania Firmino for their helpful discussions regarding the chemometrics analysis described in this article. O.U. acknowledges YÖK (Higher Education Council of Turkey) for full financial support to his postdoctoral research.

## Appendix A. Supplementary material

Table S1, with the definition of the symmetry coordinates used in the normal coordinate analyses performed on CS, TS and non-planar TS. Supplementary data associated with this article can be found, in the online version, at <http://dx.doi.org/10.1016/j.saa.2013.10.050>.

## References

- [1] D.H. Waldeck, Chem. Rev. 91 (1991) 415–436.
- [2] H. Meier, Angew. Chem. 31 (1992) 1399–1420.
- [3] T. Arai, K. Tokumaru, Chem. Rev. 93 (1993) 23–29.
- [4] D.G. Whitten, Acc. Chem. Res. 26 (1993) 502.
- [5] H. Görner, H.J. Kuhn, Adv. Photochem. 19 (1995) 1–117.
- [6] W. Fuss, C. Kosmidis, W.E. Schmid, S.A. Trushin, Angew. Chem. Int. Ed. 43 (2004) 4178–4182.
- [7] F. Hide, M.A. Diaz-Garcia, B.J. Schwartz, M.R. Andersson, Q. Pei, A.J. Heeger, Science 273 (1996) 1833–1836.
- [8] H. Suzuki, Bull. Chem. Soc. Jpn. 33 (1960) 379–388.
- [9] J. Bernstein, Spectrochim. Acta A 29 (1973) 147–149.
- [10] K. Fuke, S. Sakamoto, M. Ueda, M. Itoh, Chem. Phys. Lett. 74 (1980) 546–548.
- [11] G. Hohlneicher, B. Dick, J. Photochem. 27 (1984) 215–231.
- [12] T. Ni, R.A. Caldwell, L.A. Melton, J. Am. Chem. Soc. 111 (1989) 457–464.
- [13] H. Petek, K. Yoshihara, Y. Fujiwara, Z. Lin, J.H. Penn, J.H. Frederick, J. Phys. Chem. 94 (1990) 7539–7543.
- [14] J. Saltiel, A.S. Waller, D.F. Sears Jr., J. Am. Chem. Soc. 115 (1993) 2453–2465.
- [15] G. Hohlneicher, R. Wrzal, D. Lenoir, R. Frank, J. Phys. Chem. A 103 (1999) 8969–8975.
- [16] M. Oelgemöller, B. Brem, R. Frank, S. Schneider, D. Lenoir, N. Hertkorn, Y. Origane, P. Lemmen, J. Lex, Y. Inoue, J. Chem. Soc., Perkin Trans. 2 (2) (2002) 1760–1771.
- [17] J.A. Syage, P.M. Felker, A.H. Zewail, J. Chem. Phys. 81 (1984) 4685–4705.
- [18] J.A. Syage, P.M. Felker, A.H. Zewail, J. Chem. Phys. 81 (1984) 4706–4723.
- [19] J.S. Baskin, L. Bañares, S. Pedersen, A.H. Zewail, J. Phys. Chem. 100 (1996) (1933) 11920–11921.
- [20] S. Takeuchi, S. Ruhman, T. Tsuneda, M. Chiba, T. Taketsugu, T. Tahara, Science 322 (2008) 1073–1077.
- [21] M. Sajadi, A.L. Dobryakov, E. Garbin, N.P. Ernsting, S.A. Kovalenko, Chem. Phys. Lett. 489 (2010) 44–47.
- [22] J.H. Frederick, Y. Fujiwara, J.H. Penn, K. Yoshihara, H. Petek, J. Phys. Chem. 95 (1991) 2845–2858.
- [23] J. Quenneville, T.J. Martínez, J. Phys. Chem. A 107 (2003) 829–837.
- [24] Y. Amatatsu, Chem. Phys. Lett. 314 (1999) 364–368.
- [25] R. Improta, F. Santoro, J. Phys. Chem. A 109 (2005) 10058–10067.
- [26] M.J. Bearpark, F. Bernardi, S. Clifford, M. Olivucci, M.A. Robb, T. Vreven, J. Phys. Chem. A 101 (1997) 3841–3847.
- [27] N. Minezawa, M.S. Gordon, J. Phys. Chem. A 115 (2011) 7901–7911.
- [28] Y. Dou, R.E. Allen, J. Chem. Phys. 119 (2003) 10658–10666.
- [29] D.L. Beveridge, H.H. Jaffé, J. Am. Chem. Soc. 87 (1965) 5340–5346.
- [30] D.C. Todd, G.R. Fleming, J.M. Jean, J. Chem. Phys. 97 (1992) 8915–8925.
- [31] V. Molina, M. Merchán, B.O. Roos, Spectrochim. Acta A 55 (1999) 433–446.
- [32] M. Traetteberg, E.B. Frantsen, J. Mol. Struct. 26 (1975) 69–76.
- [33] M. Traetteberg, E.B. Frantsen, F.C. Mijlthoff, A. Hoekstra, J. Mol. Struct. 26 (1975) 57–68.
- [34] C. Dietl, E. Papastathopoulos, P. Nicklaus, R. Improta, F. Santoro, G. Gerber, Chem. Phys. 310 (2005) 201–211.
- [35] A. Hoekstra, P. Meertens, A. Vos, Acta Crystallogr. B 31 (1975) 2813–2817.
- [36] K. Ogawa, J. Harada, S. Tomoda, Acta Crystallogr. B 51 (1995) 240–248.
- [37] H. Watanabe, Y. Okamoto, K. Furuya, A. Sakamoto, M. Tasumi, J. Phys. Chem. A 106 (2002) 3318–3324.
- [38] G. Orlandi, L. Gagliardi, S. Melandri, W. Caminati, J. Mol. Struct. 612 (2002) 383–391.
- [39] M.L. Freile, S. Risso, A. Curaqueo, M.A. Zamore, R.D. Enriz, J. Mol. Struct. (Theochem.) 731 (2005) 107–114.
- [40] P.D. Chowdhary, T.J. Martínez, M. Gruebele, Chem. Phys. Lett. 440 (2007) 7–11.
- [41] S.P. Kwasniewski, L. Claes, J.-P. Francois, M.S. Deleuze, J. Chem. Phys. 118 (2003) 7823–7836.
- [42] A. Bree, M. Edelson, Chem. Phys. 51 (1980) 77–88.
- [43] J.F. Arenas, I.L. Tocon, J.C. Otero, J.I. Marcos, J. Phys. Chem. 99 (1995) 11392–11398.
- [44] C.H. Choi, M. Kertesz, J. Phys. Chem. A 101 (1997) 3823–3831.
- [45] W.-Y. Chiang, J. Lanne, J. Chem. Phys. 100 (1995) 8755–8767.
- [46] J.M. Robertson, I. Woodward, Proc. R. Soc. London A 162 (1937) 568–583.
- [47] C.J. Finder, M.G. Newton, N.L. Allinger, Acta Crystallogr. B 30 (1974) 411–415.
- [48] J. Bernstein, Acta Crystallogr. B 31 (1975) 1268–1271.
- [49] J.A. Bouwstra, A. Schouten, J. Kroon, Acta Crystallogr. C 40 (1984) 428–431.
- [50] M. Edelson, A. Bree, Chem. Phys. Lett. 41 (1976) 562–564.
- [51] G. Celebre, G. De Luca, M.E. Di Pietro, J. Phys. Chem. B 116 (2012) 2876–2885.
- [52] D. Tzeli, G. Theodorakopoulos, I.D. Petsalakis, D. Ajami, J. Rebeck Jr., J. Am. Chem. Soc. 134 (2012) 4346–4354.
- [53] B.P. Kar, N. Ramanathan, K. Sundararajan, K.S. Viswanathan, J. Mol. Struct. 994 (2011) 364–370.
- [54] M.J. Frisch, G.W. Trucks, H.B. Schlegel, G.E. Scuseria, M.A. Robb, J.R. Cheeseman, J.A. Montgomery, Jr., T. Vreven, K.N. Kudin, J.C. Burant, J.M. Millam, S.S. Iyengar, J. Tomasi, V. Barone, B. Mennucci, M. Cossi, G. Scalmani, N. Rega, G.A. Petersson, H. Nakatsuji, M. Hada, M. Ehara, K. Toyota, R. Fukuda, J. Hasegawa, M. Ishida, T. Nakajima, Y. Honda, O. Kitao, H. Nakai, M. Klene, X. Li, J.E. Knox, H.P. Hratchian, J.B. Cross, V. Bakken, C. Adamo, J. Jaramillo, R. Gomperts, R.E. Stratmann, O. Yazyev, A.J. Austin, R. Cammi, C. Pomelli, J.W. Ochterski, P.Y. Ayala, K. Morokuma, G.A. Voth, P. Salvador, J.J. Dannenberg, V.G. Zakrzewski, S. Dapprich, A.D. Daniels, M.C. Strain, O. Farkas, D.K. Malick, A.D. Rabuck, K. Raghavachari, J.B. Foresman, J.V. Ortiz, Q. Cui, A.G. Baboul, S. Clifford, J. Cioslowski, B.B. Stefanov, G. Liu, A. Liashenko, P. Piskorz, I. Komaromi, R.L. Martin, D.J. Fox, T. Keith, M.A. Al-Laham, C.Y. Peng, A. Nanayakkara, M. Challacombe, P.M.W. Gill, B. Johnson, W. Chen, M.W. Wong, C. Gonzalez, J.A. Pople, Gaussian 03, Revision C.02, Gaussian, Inc.: Wallingford CT, 2004.
- [55] A.D. Becke, Phys. Rev. A 38 (1988) 3098–3100.

- [56] C.T. Lee, W.T. Yang, R.G. Parr, *Phys. Rev. B* 37 (1988) 785–789.
- [57] A.D. McLean, G.S. Chandler, *J. Chem. Phys.* 72 (1980) 5639–5648.
- [58] F. Weinhold, C.R. Landis, *Valency and Bonding. A Natural Bond Orbital Donor–Acceptor Perspective*, Cambridge University Press, New York, 2005.
- [59] A.E. Reed, L.A. Curtiss, F. Weinhold, *Chem. Rev.* 88 (1988) 899–926.
- [60] J. H. Schachtschneider, F. S. Mortimer, *Vibrational Analysis of Polyatomic Molecules. VI. FORTRAN IV Programs for Solving the Vibrational Secular Equation and for the Least-Squares Refinement of Force Constants*. Project No. 31450. Structural Interpretation of Spectra; Shell, Development Co. 1969.
- [61] R Core Team (2012). R: A Language and Environment for Statistical Computing. R Foundation for Statistical Computing, Vienna, Austria. ISBN 3-900051-07-0, <<http://www.R-project.org/>>.
- [62] I.D. Reva, S.G. Stepanian, L. Adamowicz, R. Fausto, *Chem. Phys. Lett.* 374 (2003) 631–638.
- [63] L. Pauling, J. Sherman, *J. Chem. Phys.* 1 (1933) 606–617.
- [64] R.S. Mulliken, R.G. Parr, *J. Chem. Phys.* 19 (1951) 1271–1278.